Final Report

Development of a Thermionic Magnicon Amplifier at 11.4 GHz

Interagency Agreement No. DE–AI–02–94ER40861

Report No. DOE/ER/40861–7

Submitted to: U.S. Department of Energy

Submitted by: Plasma Physics Division
Naval Research Laboratory
Washington, DC 20375–5346

Investigators: Dr. Steven H. Gold
Dr. Arne W. Fliflet

Report Period: 16 May 1995 – 15 May 2001

DISCLAIMER

Outline

I. Executive Summary

This is the final report on the research program entitled "Development of a Thermionic Magnicon Amplifier at 11.4 GHz," which was carried out by the Plasma Physics Division of the Naval Research Laboratory (NRL) under Interagency Agreement DE–AI02–94ER40681 between NRL and the U.S. Department of Energy (DoE). The purpose of this program was to develop a high–power, long–pulse, repetitively–pulsed, frequency–doubling X–band magnicon amplifier for potential application to future linear colliders. The final design parameters were 61 MW at 11.424 GHz, 59 dB gain, and 59% efficiency, with a 1–μs output pulse and a repetition rate of up to 10 Hz. This program began on 16 May 1995 and ended on May 15, 2001. It was replaced by a new Interagency Agreement entitled "Dielectric–Loaded Accelerator and Active Pulse Compressor Development at 11.424 GHz," in which the NRL Magnicon Facility will be used to develop and test other accelerator technologies at 11.424 GHz.

Through most of this program, NRL has worked closely with an industrial partner, Omega–P, Inc. of New Haven, CT. Omega–P, Inc. was awarded a Phase II SBIR grant for magnicon research by the Department of Energy in May 1996. This led to the establishment of a formal Cooperative Research and Development Agreement with NRL (NCRADA–NRL–96–108) to jointly develop a high–power 11.424–GHz magnicon amplifier tube. This CRADA was extended through 31 December 1999, and was also expanded to cover the planned testing of a 10× active microwave pulse compressor using the high power 11.424–GHz output from the experimental magnicon tube. The formal CRADA expired on that date, but close collaboration continued through the end of the Agreement.

Previous progress reports covered the period from the beginning of the program through 31 December 2000. This final report will summarize the key elements of the previous reports and detail the additional progress through the formal end of the Agreement.

II. Introduction

The magnicon [1–4] is an advanced high–power "scanning–beam," or deflection–modulated microwave amplifier tube intended for use in powering future high–gradient linear accelerators, such as the proposed Stanford Linear Accelerator Center (SLAC) TeV linear collider concept known as the Next Linear Collider (NLC). The frequency chosen for the NLC is 11.424 GHz. SLAC has developed high–power klystrons at this frequency with powers as high as 75 MW in a ~3–μs pulse at efficiencies exceeding 50%. These klystrons are the leading candidate to power the NLC. The magnicon is a possible competitor to these klystrons. Its potential advantages include: 1) higher efficiency, because of the use of a synchronous interaction that does not require beam bunching; 2) higher power per tube, because of the potential for operating at higher perveance without loss of efficiency; 3) longer output pulse lengths (which would permit higher levels of microwave pulse compression to be employed), because of the lower fields in the output cavity and the lack of current interception on the rf circuit should reduce the likelihood for rf breakdown; and 4) insensitivity to load mismatches, because the output cavity interaction is transverse, rather than axial, and thus cannot easily reflect electrons. It is also believed that the magnicon can be extrapolated to higher frequencies than the klystron, for a given operating power level, because the output cavity is a single fast–wave cavity, similar to that used in a gyrotron, rather than a multisection traveling–wave output structure, and because the deflection cavities can be larger than klystron bunching cavities by operating at lower frequency and in a higher–order mode.

A Russian magnicon program has existed for a number of years at the Budker Institute for Nuclear Physics (INP) in Novosibirsk, Russia. In recent years, the focus of that program has been at 7 GHz. They have developed a device that produces 55 MW in a 1.1–μs pulse at 56% efficiency, with 72 dB gain, using a 427–kV, 230–A electron beam from a high–convergence Pierce electron gun [5]. Some of the principal scientists from that program have been involved in the NRL program through the collaboration with Omega–P, Inc. An earlier single–shot magnicon experiment at NRL, employing an explosive–emission cathode driven by a Marx generator to produce the electron beam, produced 14 MW at 11.12 GHz at 10% efficiency, using a 650–keV, 225–A electron beam [6]. A program to produce a high–power, frequency–tripling 34–GHz magnicon amplifier is also under way at Omega–P, Inc [7]. The broad goal of the program in the Beam Physics Branch of the Plasma Physics Division at NRL was to produce the first high–power, repetitively–pulsed magnicon operating in X–band, and the first working magnicon in the U.S. The specific aim was to produce ~60 MW at 11.424 GHz in a 1–μs pulse with a gain of 59 dB and an efficiency of ~60%.

In the NRL 11.424–GHz magnicon (see Fig. 1), a ~470–keV, 220–A, ~2–mm–diam. magnetized pencil beam from an ultrahigh–convergence electron gun transits a drive cavity containing a rotating TM_{110} mode generated by an external rf source. The rotating rf magnetic field of the TM_{110} mode converts a small fraction of the beam axial momentum into transverse momentum (Larmor motion) about the applied axial magnetic field. The beam then enters a sequence of gain cavities, where the transverse beam momentum induces amplified rf fields that further deflect the beam, producing a progressively higher fraction of transverse momentum. This process proceeds until the electrons exiting the final two deflection cavities, known as penultimate cavities, have an α>1, where α is the ratio of transverse to parallel momentum. Unlike the gain cavities of the klystron, the gain cavities of the magnicon are not used to create bunching, but rather to amplify the transverse motion of the beam—because of the scanning–beam interaction using rotating rf cavity modes, the electron motion is synchronous with the phase of the rf fields in each of the magnicon cavities, beginning with the drive cavity.

As a result of the phase–synchronous transverse deflection of the electron beam as a whole, the beam electrons entering the output cavity execute Larmor motion *whose entry point and guiding center rotate in space about the cavity axis at the drive frequency.* In the output cavity, the beam drives a cyclotron–resonant fast–wave interaction that extracts

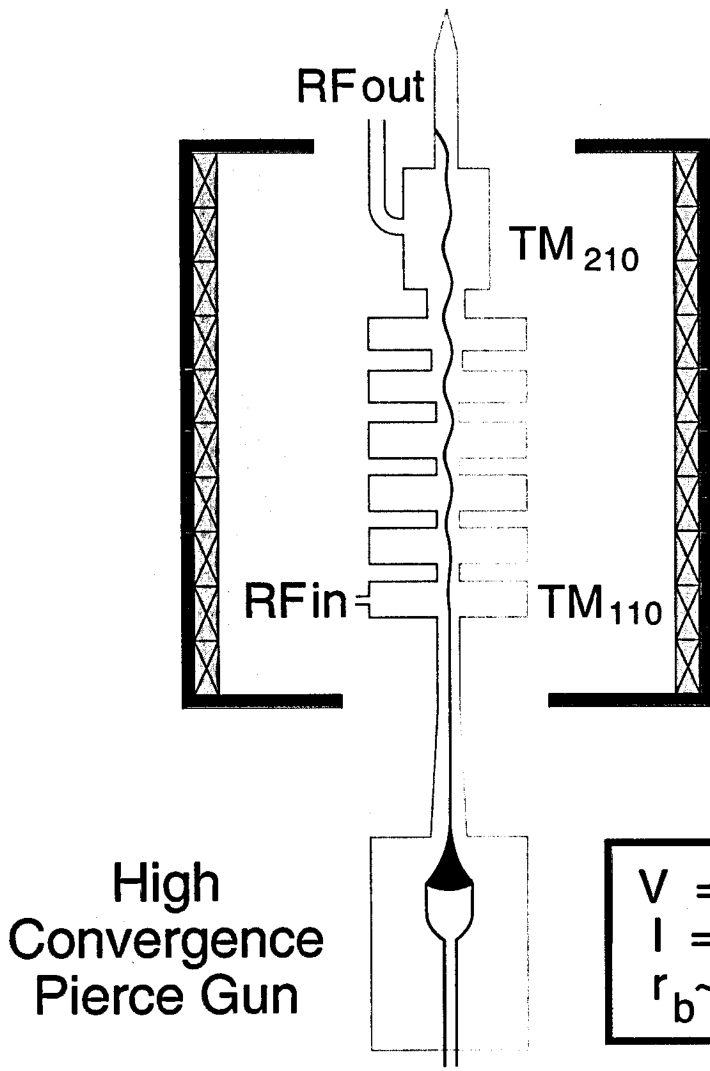

Design Parameters

Frequency	11.424 GHz
Power	61 MW
Pulse width	1 μsec
Repetition rate	10 Hz
Efficiency	59 %
Drive frequency	5.712 GHz
Gain	59 dB

$V = 470$ kV
$I = 220$ A
$r_b \sim 1$ mm

Figure 1. Schematic diagram of the NRL X-band magnicon amplifier experiment

principally the transverse beam momentum. This interaction is analogous to that of a fundamental–cyclotron–harmonic gyroklystron, although magnicons typically use TM rather than TE output–cavity modes. However, unlike the situation in an ordinary gyroamplifier, the electrons in the magnicon arrive in the output cavity coherently gyrophased. This provides for optimum energy transfer to a mode of the output cavity that rotates synchronously with the deflection cavity modes, and makes possible very high efficiencies. However, maintaining a tight electron phase bunch in the magnicon output cavity requires the use of a good quality, small–radius electron beam in the deflection cavities. The phase–synchronous interaction in the output cavity can take place at either the fundamental or a higher harmonic of the drive frequency. For an 11.424 GHz magnicon, it is convenient to operate the output cavity at twice the frequency of the deflection cavities, but still in the first harmonic of the cyclotron frequency. For that reason, the drive signal in the NRL magnicon is at 5.712 GHz.

III. Overview of the Program

The goal of this program was to develop a prototype high–power 11.424–GHz magnicon amplifier as an alternative to klystrons to power future linear colliders. This required the development of a ultrahigh–convergence electron gun, a suitable microwave circuit, and a number of other unique components, including a special beam analyzer to measure the characteristics of the electron gun, and a special compact bakable gate valve. The entire device had to be designed for operation at $\sim 10^{-8}$ Torr. This required all metal and ceramic construction and engineering comparable to that carried out at SLAC on the X–band klystrons. At the conclusion of the Interagency Agreement, the magnicon was undergoing final conditioning, and had already been used to carry out the first tests of a high–power microwave active pulse compressor using a plasma switch.

This Section of the report provides an overview of the principal components of the magnicon experiment. Section IV will present a detailed summary of the experimental work during the period from 1 January 2001 through 15 May 2001.

A. The Laboratory

Figure 2 shows the layout of the magnicon laboratory. This scale drawing illustrates the position of the modulator, tube socket, experimental platform, and magnet power supplies within the concrete shielding wall. An X–ray shielding wall encloses the experimental area, which is under radiation monitoring, and the entry gate is interlocked to prevent entry when the magnicon is operating.

A high–power electron–gun modulator is located inside the shielding wall. A large metal experimental stand, consisting of a 6' high, 5'x6' platform with guard rails, is centered over the modulator gun socket. This platform gives access to all parts of the magnicon experiment, and also supports diagnostics and lead x–ray shielding. Cable trays are in place extending outwards

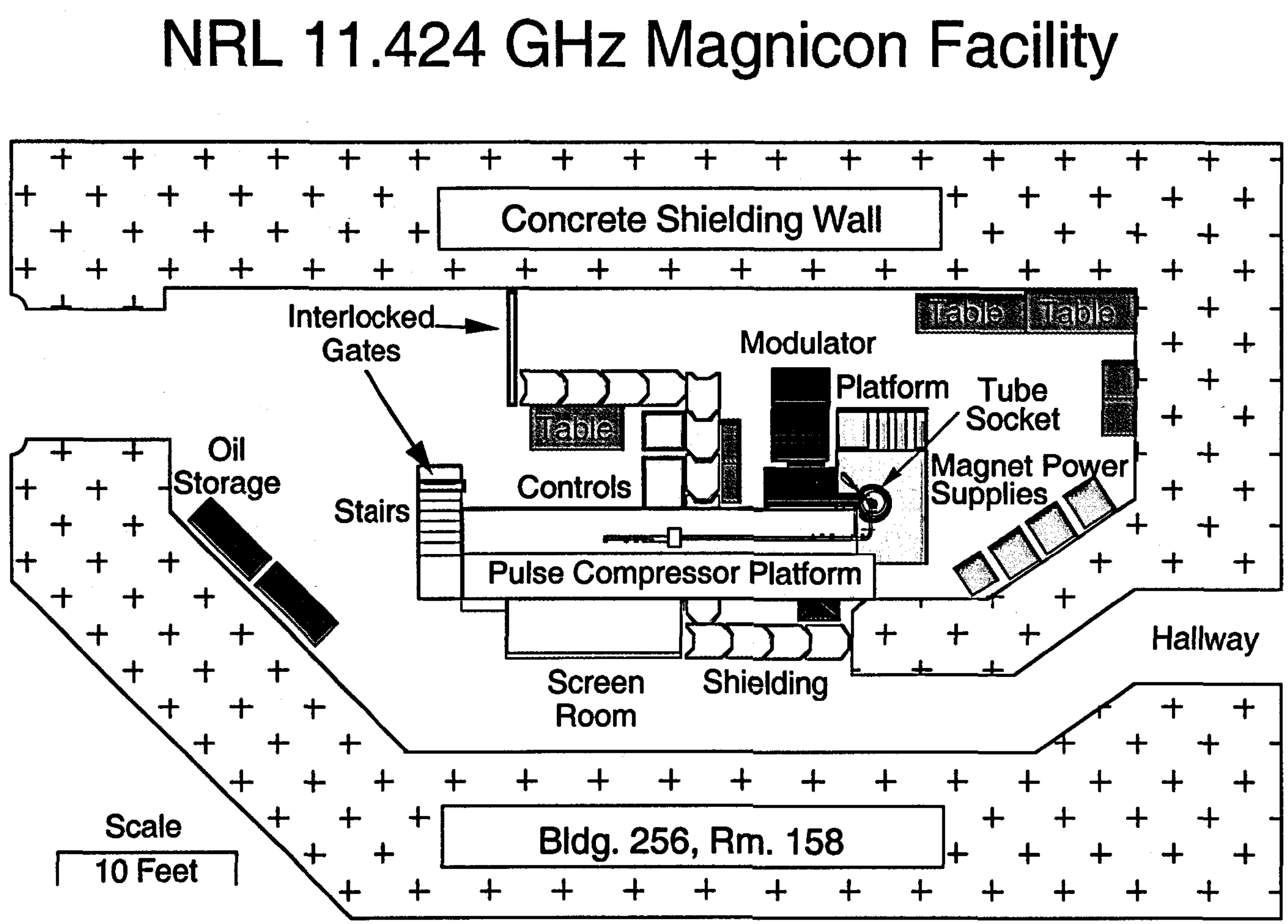

Figure 2. Scale drawing of the NRL 11.424-GHz magnicon facility

from the platform to support the heavy magnet power supply cables and cooling water hoses, and also to support signal cables leading from the experimental area to the screen room. A set of stairs provides secure access to the platform. A second raised platform was built for high-power microwave pulse compressor experiments [8] that will be carried out at NRL in collaboration with Omega–P, Inc. and the Institute of Applied Physics (IAP) in Nizhny–Novgorod, Russia. This platform is 5'x24', mounted 8' off the floor, and passes over the concrete shielding wall and over a portion of the screen room. It is accessible both from the magnicon platform and from the experimental control area. One arm of the microwave output will be connected by waveguide components to the front of the pulse compressor, which is already in place on the second platform.

A screen room and control area are installed outside of the shielding. The screen room contains the rf–drive system, including an rf sweep oscillator, frequency counter, and 1–kW C–band TWT driver. It also houses controllers for the five ion pumps attached to the magnicon vacuum, microwave diagnostic components, and 16 fast digital oscilloscope channels.

B. The Modulator

The magnicon electron gun is powered by a 500–kV, 250–A, 10–Hz soft–tube modulator originally built in 1990 by Beta Development Corporation, now Titan Beta, Inc. A variety of modifications and improvements were made to adapt the modulator to the electron gun, to improve its reliability, and to improve its calibration to the precision required for the development of technology for accelerator applications. The modulator is currently operating reliably at voltages up to 480 kV.

C. The Magnicon Magnet and Power Supplies

The magnicon magnet is a water–cooled cw magnet with an iron yoke that was designed to be fully matched to the magnicon electron gun. A 60–kW heat–exchanger, cooled by building chilled water, removes the ohmic heat from the magnet. Chilled water from the heat exchanger is sent to a cooling–water manifold that distributes it to each of the separate magnet coils. (Chilled water is also circulated through the electron–beam collector and the anode of the electron gun, and around the outside of the penultimate cavities.)

Three 600–A, 40–V power supplies and one 300–A, 40–V power supply, remotely operated from the control area, are used to drive the 10 magnet coils. Each of the 600–A power supplies is powered by a separate 480–V, 60–A, 3–phase AC circuit. The magnet power supplies are interlocked to the water flow to avoid magnet overheating in the event of a chilled–water failure. The coils are wired in sets, with coils #1–4 powered by the first 600–A supply, #5 and #6 by the second 600–A supply, #7 by the 300–A supply, and #8–10 by the third 600–A supply. In order to create a dip in the magnetic field in the vicinity of the penultimate cavity, the current through coil #7 runs in the opposite sense from the current through the remaining coils. There is also a bucking coil, to cancel out leakage fields on the cathode, that requires up to 5 A to operate, and two steering coils, around the upper portion of the electron gun, that each require up to 5 A to operate. Three low–current power supplies are in place to power the bucking and steering coils.

D. The Electron Gun

The electron gun is a special ultrahigh–convergence Pierce gun that was designed jointly by Omega–P, Inc. and Litton Electron Devices, and manufactured by Litton [9,10]. The original design called for a 500–kV, 210–A electron beam (microperveance 0.59) that focuses down to a radius of 0.75 mm at the anode. However, some fabrication errors were made when the gun was manufactured, and the final measured beam size was ~2.2 mm at a perveance of 0.63 μperv, but with noticeable asymmetry. The history of the gun, and a description of the original electron beam measurements, is presented in Ref. [11]. The electron gun connects to the remainder of the magnicon experiment through a special gate valve [12], that permits changes to be made in the experimental setup without bringing the gun up to atmospheric pressure.

The electron gun was rebuilt by Calabazas Creek Research, Inc. following a collector failure on 3 November 1999 that produced a water leak into the vacuum, poisoning the cathode. At that time, the cathode and focus electrode assemblies were redesigned to correct the previous asymmetry. The new design uses ceramic balls to center the cathode stalk within the focus electrode (see Fig. 3), in place of a ceramic ring that was found to have cracked due to expansion of the cathode stalk during normal operation. The rebuilt gun has a perveance of 0.68 μperv, somewhat higher than the 0.63 μperv design value for the rebuilt gun. This indicates that the cathode–anode gap is ~1 mm smaller than the design value, indicating that the cathode stalk expansion at operating temperature was underestimated. Detailed measurements of the beam were carried out using the Beam Analyzer (see Section III.G.) They showed a slightly asymmetric beam (see Fig. 4), but much less so than before the gun repair. The mean beam diameter is ~2 mm, somewhat smaller than for the Litton–built gun. However, there is residual scalloping that is attributed to the slightly higher gun perveance than the design value. Simulations suggest that as a result of the higher beam current, the beam reaches focus too soon, and as a result is not matched properly into the field of the magnicon magnet. Figure 5 shows a comparison of the simulated beam edge as a function of z with the results of the beam measurements.

E. The Cavities

The magnicon circuit has a drive cavity, three gain cavities, and two penultimate cavities, all operating in the TM_{110} mode at 5.712 GHz, followed by an output cavity operating at 11.424 GHz in the TM_{210} mode. The circuit, is fabricated from OFHC copper, with the cavity surfaces diamond–turned and the assembly diffusion bonded together. Each deflection cavity has two miniconflat flanges, separated by 90°, to allow the insertion of coupling loops to measure the two

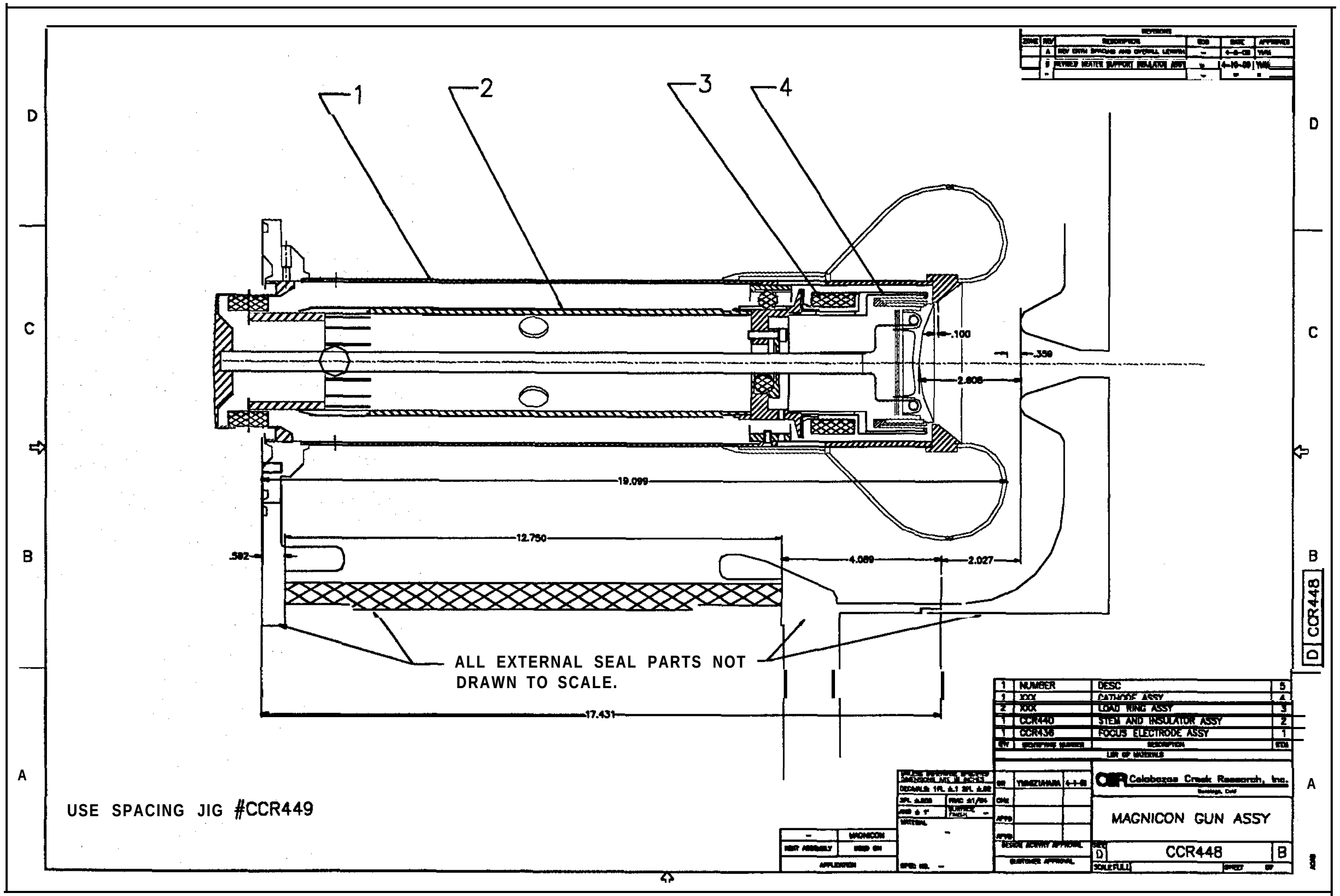

Figure 3. Scale drawing of rebuilt cathode stalk for magnicon electron gun

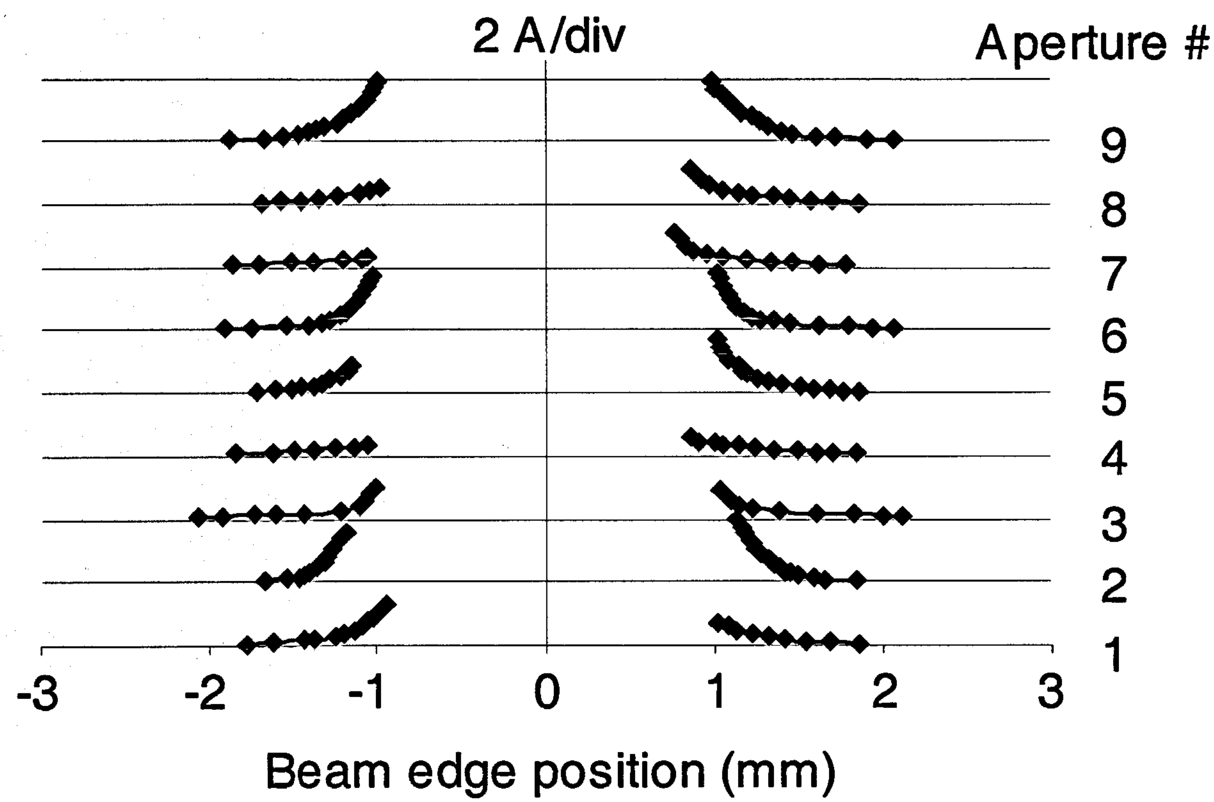

Figure 4. Beam edge current interception measurements

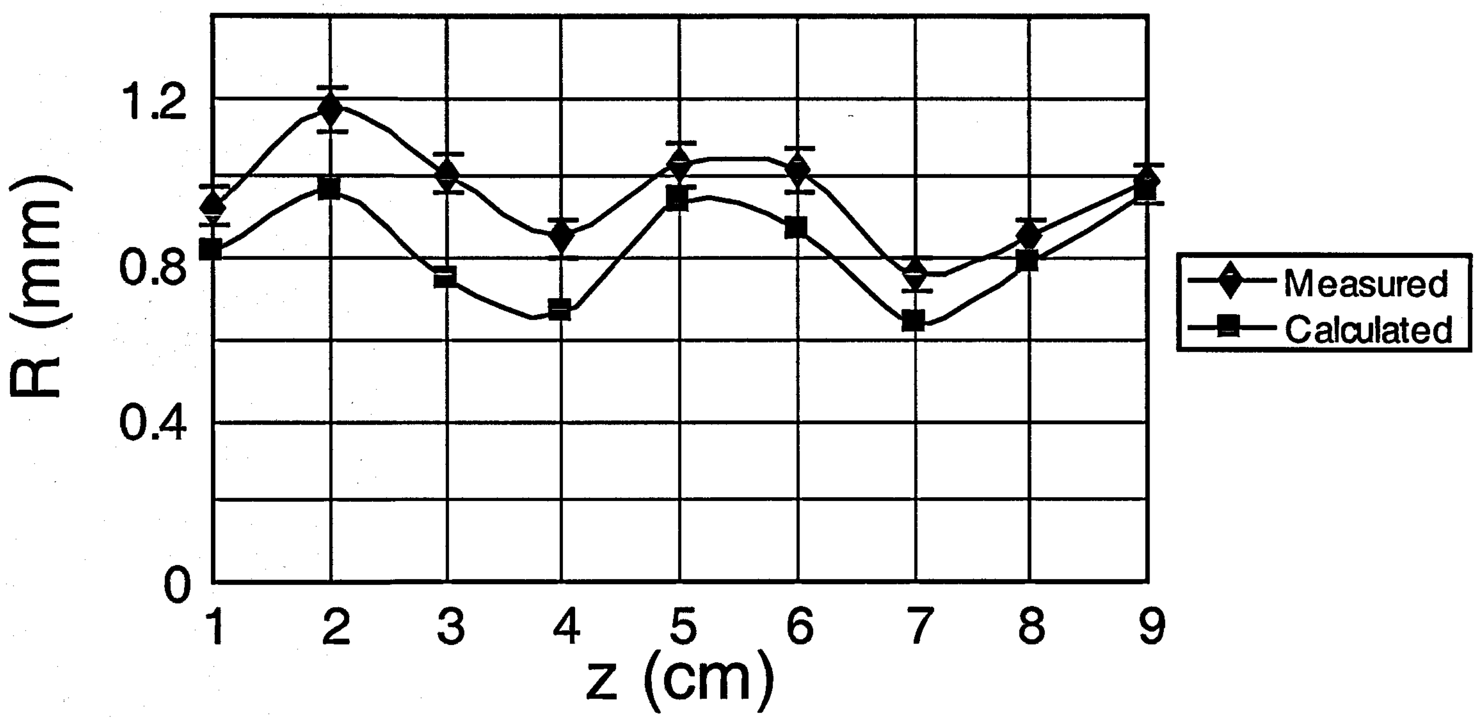

Figure 5. Comparison of measured and predicted beam envelope (95% of current)

orthogonal polarizations of the circularly–polarized operating mode. For the drive cavity, the second insertion point is used for a tuning stub to compensate for the coupling loop, while for the remaining cavities, only one loop is used to sample the rotating mode. The loops were calibrated using a loop inserted from the end of the cavity assembly. The output cavity uses two WR–90 waveguides, 135° apart and connected by rectangular SLAC high–power flanges, to extract both components of the rotating TM_{210} mode. The completed circuit is shown in Fig. 6.

F. The Collector

The original collector design included an inverted Cu inner cone enclosed by a double water jacket (see Fig. 7). The outer water jacket brings cooling water down to the bottom end of the cone, and the inner jacket carries the water over the outer surface of the cone in order to remove the deposited heat. The end of the collector is always positioned outside of the axial field magnet, so that space charge effects will spread the beam over a large area of the collector cone surface. Electron trajectories and energy deposition were modeled for all cases, and the collector designed to provide adequate heat dissipation. The cone and water jacket were electrically isolated from the outer portion of the vacuum enclosure, so that direct measurements could be made of the beam current deposited in the collector. This collector failed after more than 2×10^6 pulses due to the formation of a sub–mm hole through ~1 cm of copper at the precise center of the collector cone and into the enclosing water jacket. This failure was attributed to ion focusing, due to inadequate vacuum conditions during the condition process. This resulted in a small fraction of the 200–A beam current pinching at the end of the collector, and progressively damaging the copper cone.

While a complete understanding of the physics that resulted in collector damage due to ion focusing of the electron beam is lacking, the solution to the problem of ion focusing in the collector seemed to be straightforward in concept, and was addressed in a redesign and reengineering of the collector cone. The first step was to improve the vacuum conductance

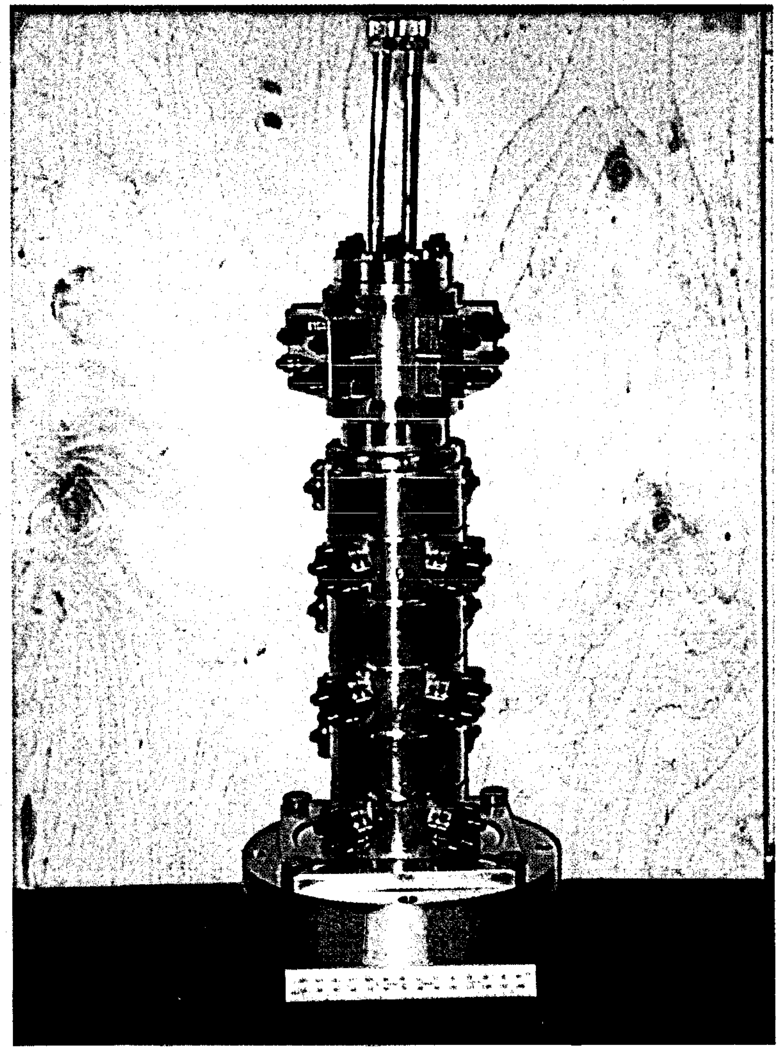

Figure 6. Photograph of the magnicon cavity assembly

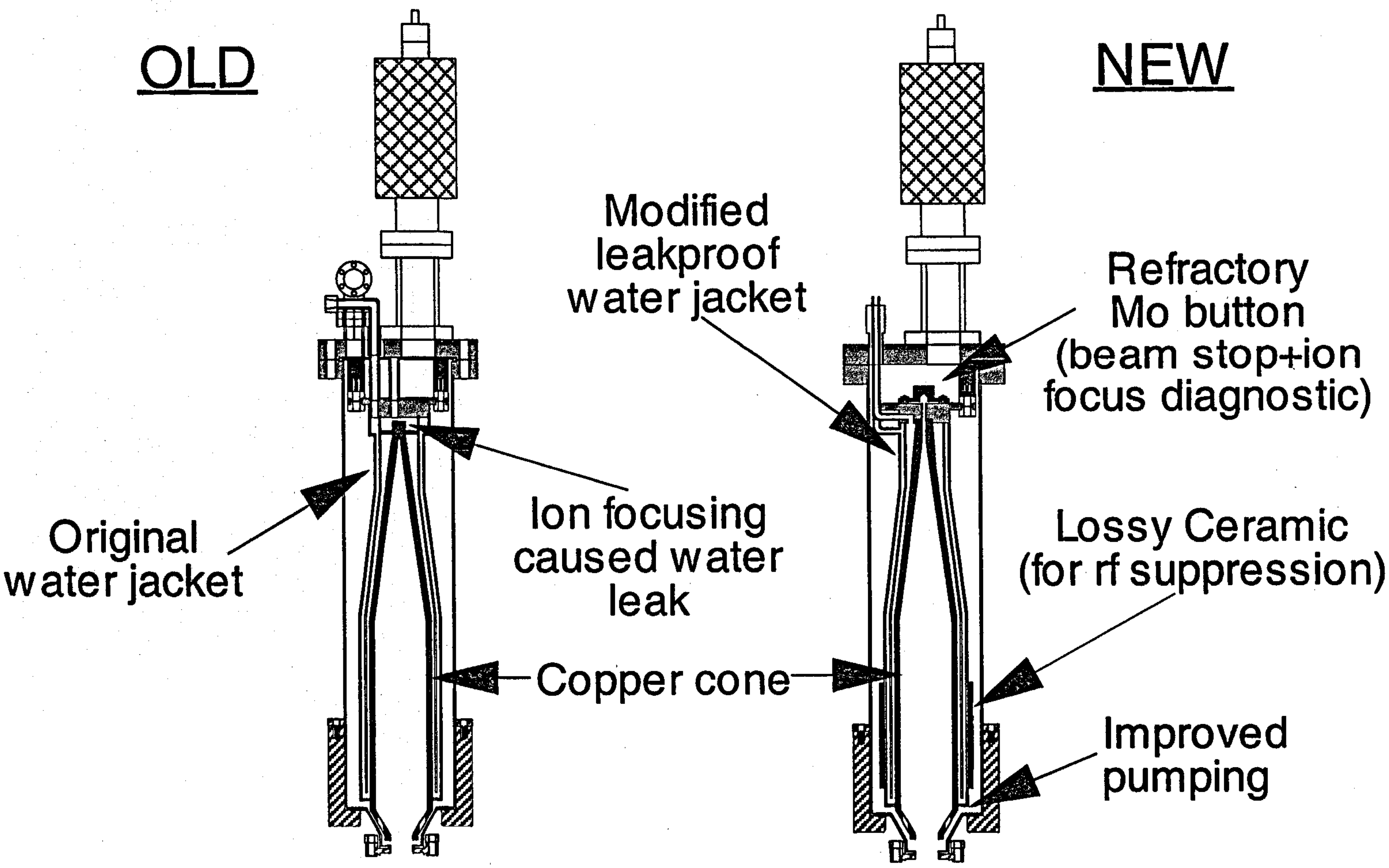

Figure 7. Scale drawings of old and new collector designs

between the interior of the collector cone and the 8–liter ion pump located at the end of the collector vacuum housing by increasing the size of the pumping slit at the bottom of the cone. This was designed to help reduce the background pressure of neutral gas molecules, which permits ion focusing to occur. However, additional measures were taken, first to mitigate the potential damage should ion focusing occur, and second to monitor its occurrence, in order to avoid operating parameters that induce it.

The old collector design had a water jacket that wrapped completely around the sides and back of the collector cone. When the beam bored through the specially thickened end of the cone (~1 cm Cu), it created a leak from the water jacket directly into the vacuum system. It was the water leak, rather than the ablated copper, that caused the consequent damage to the electron gun and the vacuum system. Since the damage to the collector cone was exactly on the beam axis, the central portion of the new copper cone end was drilled out, creating a channel through which ion–focused current could pass. Behind this channel, there is an Mo insert (melting point: 2890 K), which is electrically isolated from the copper cone, but in thermal contact with it through ceramic AlN spacers. A pinched beam will thus encounter a much more refractory material than Cu (melting point: 1356 K). Moreover, even if the Mo insert were to burn through, the beam would not create a water leak, but would instead strike the end flange of the collector vacuum enclosure.

Next, because the Mo insert is electrically isolated from the remainder of the collector cone as well as from the outer vacuum jacket, current intercepted by it can be separately measured using a wire attached to the back side of the Mo button that brings the signal out of the vacuum enclosure through an electrical feedthrough. Under normal conditions, space–charge expansion of the beam will reduce the current reaching the insert approximately to zero. However, any dangerous increase in this current, indicative of ion focusing, would be immediately apparent to the magnicon operator, who can take appropriate actions, such as reducing the repetition rate or pausing to permit the vacuum pressure to recover. Figure 7 shows some of the details of the redesigned end of the collector cone.

In operation during the beam edge measurements described in Section IV, the Mo button worked as designed, showing that only ~0.3 A of current reached the cone under conditions of good vacuum. However, during the initial magnicon conditioning described in Section IV.E, gas liberated from the cavities due to rf breakdown effects could increase the pressure in the collector cone enough to collect up to 10–20 A on the button. (We have never observed a situation in which more than 10% of the instantaneous collector current reaches the button.) This information was used to moderate the magnicon repetition rate in order to minimize the button current. However, during the conditioning, the button signal began to degrade: it began to have a component looking like the derivative of the main collector cone current. A resistance measurement demonstrated that the button was no longer electrically isolated from the main copper cone, but was separated from it by only a small impedance. The collector was opened for examination in April 2001. It was determined that the problem was tracking across dielectric surfaces separating the button from the remainder of the collector cone. This problem was solved by sanding the tracks out of the ceramic, restoring the separate button and collector signals.

G. <u>The Beam Analyzer</u>

The design of the special high–vacuum electron–beam analyzer (see Fig. 8) is discussed in detail in Ref. [13]. Instead of directly intercepting the full electron beam in order to measure its size, it measures only the edges of the beam using a set of ten graphite apertures that are spaced at 1–cm intervals along the beam axis. The apertures are mounted on a rotating drum, with only one aperture in use at a time. Each aperture is translated laterally until a small fraction of the beam current is intercepted, first from one edge of the beam, and then from

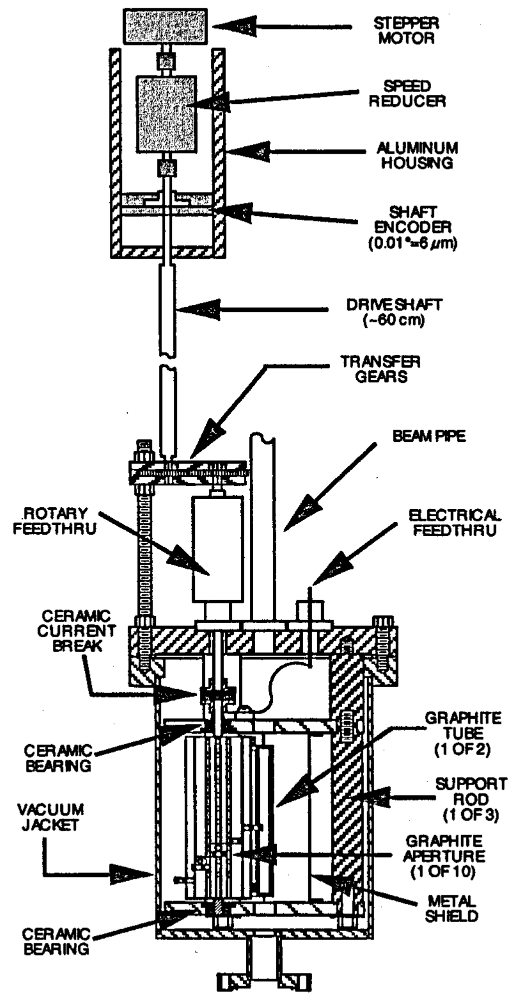

Figure 8. Electron beam measurement apparatus

the opposite edge. Measurements begin beyond the edge of the beam, and continue inward until the total intercepted current rises to several amps. Beyond this point, large amounts of gas are liberated from the aperture, making useful measurements impossible. It is important to note that since beam matching is a function of voltage, the intercepted current often differs substantially during the rise and fall of the voltage waveform. Thus, the maximum value of intercepted current that can be measured during the voltage flat–top by a particular aperture edge is often limited by higher values of intercepted current elsewhere in the pulse.

This apparatus permits the beam size to be measured and optimized as a function of the focus–electrode bias voltage and the current in the bucking and steering coils. The beam dimensions are then an input parameter into the magnicon simulation code.

H. The Magnicon Drive System

Figure 9 shows a simplified schematic of the magnicon rf drive system. A low–power sweep oscillator (Hewlett–Packard Model 8350B Sweep Oscillator, with a Model 83590A 2–20 GHz RF Plug–in) generates a tunable chirp–free cw rf seed signal of up to 100 mW. Its absolute drive frequency is monitored using an EIP Model 575 Source–Locking Microwave Counter. The seed signal is amplified by a Logimetrics Model A750 Traveling–Wave–Tube Amplifier with 1–kW pulsed output and 60–dB gain. The duration of the magnicon input pulse is controlled by varying the length of the TWT output pulse. This signal then passes through an isolator, forward and reverse directional couplers, and ~15 m of ultra–low loss Heliax cable before reaching the magnicon platform, where a transition is made to a small low–loss semi–rigid cable with SMA connectors that brings the signal to the drive cavity. There, it attaches to a Kaman bakable high–vacuum matched 50–Ω SMA rf feedthrough that has been electron–beam welded into a miniconflat flange. The feedthrough connects to a special compensated rf coupling loop that extends into the drive cavity. The center pin of the

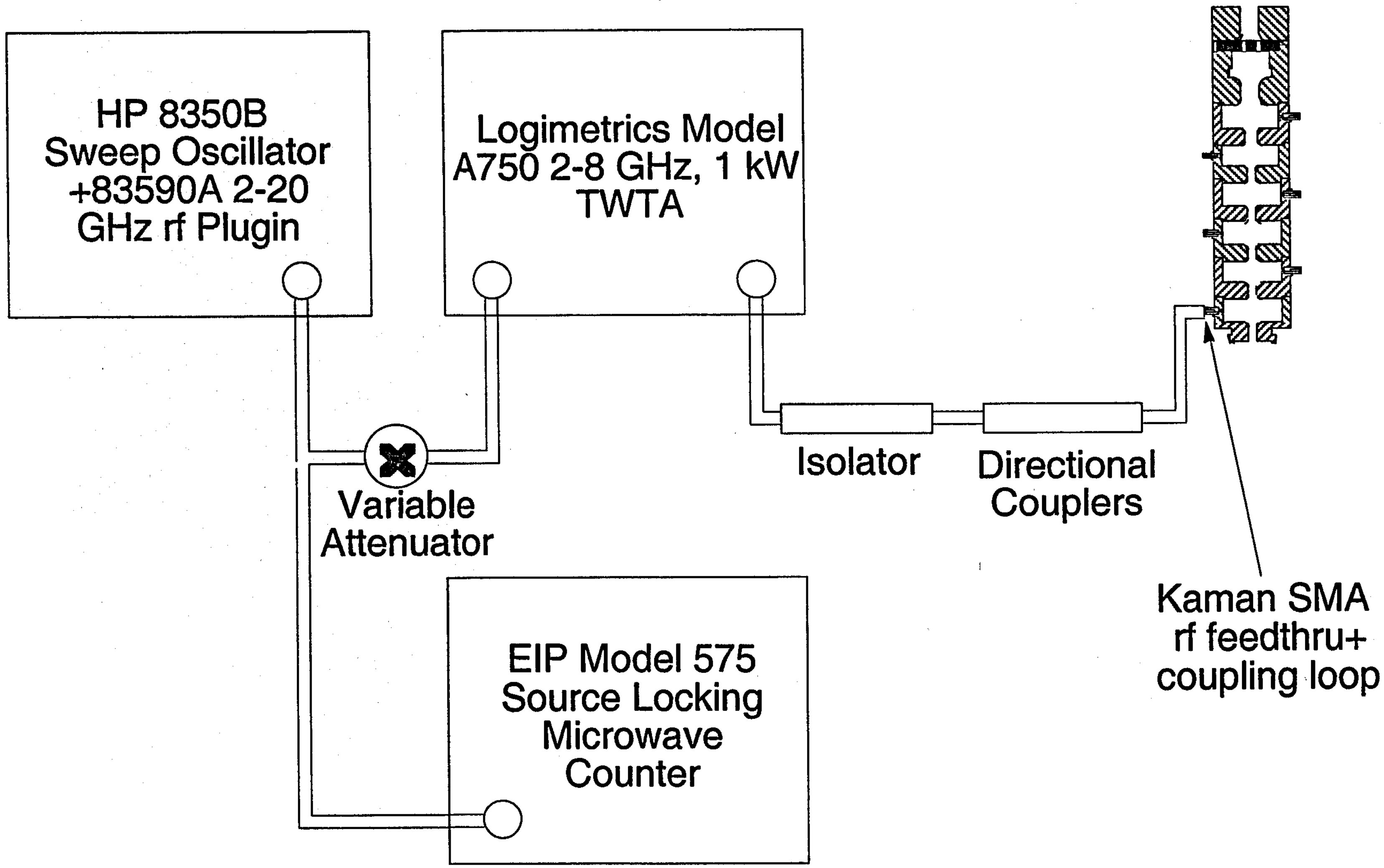

Figure 9. Schematic diagram of the magnicon rf drive system

feedthrough passes through a tunnel in the cavity wall whose diameter matches the 50–Ω impedance of the drive cable. The outer end of the center pin is threaded at 0–80, and the coupling loop has a female 0–80 thread, so that the loop extension and orientation can be adjusted. Following adjustment, the loop is spot–welded into place. A special Cu vacuum gasket maintains the tunnel diameter in the region between the miniconflat connector flange and the matching flange that is brazed to the outer wall of the cavity assembly. Simulations suggest that 75 to 150 W of drive power must to be coupled into the first cavity to drive the magnicon output to saturation under the optimal magnetic field configuration for high efficiency operation. Measurements of transmission and coupling loss indicate that this level of drive power can readily be coupled into the cavity.

I. The Magnicon Output System

Figure 10 shows a top view of the magnicon output. The microwave power is extracted from the output cavity through two WR–90 waveguides emerging from the sides of the output cavity with an angular separation of 135°. These output waveguides are bent vertically immediately outside the cavity, and then bent horizontally, to cross over the top of the collector. Both waveguide arms have: 1) separate pumping by an ion pump, via a pump–out tee, 2) a bi–directional coupler to monitor the power and pulse shape (and to observe reflections from the load), and 3) a high–peak–power water–cooled load to absorb the power and to measure the deposited energy. For this purpose, SLAC–built pump–out tees, 55–dB directional couplers, and high–power loads were used.

Because of the very high peak power of up to 30 MW expected per waveguide in a 1–μs pulse, and the difficulty of obtaining matched microwave windows that can withstand this power level without breakdown, we chose to carry out the initial conditioning and power measurements in a windowless configuration, in which the output components share the main magnicon

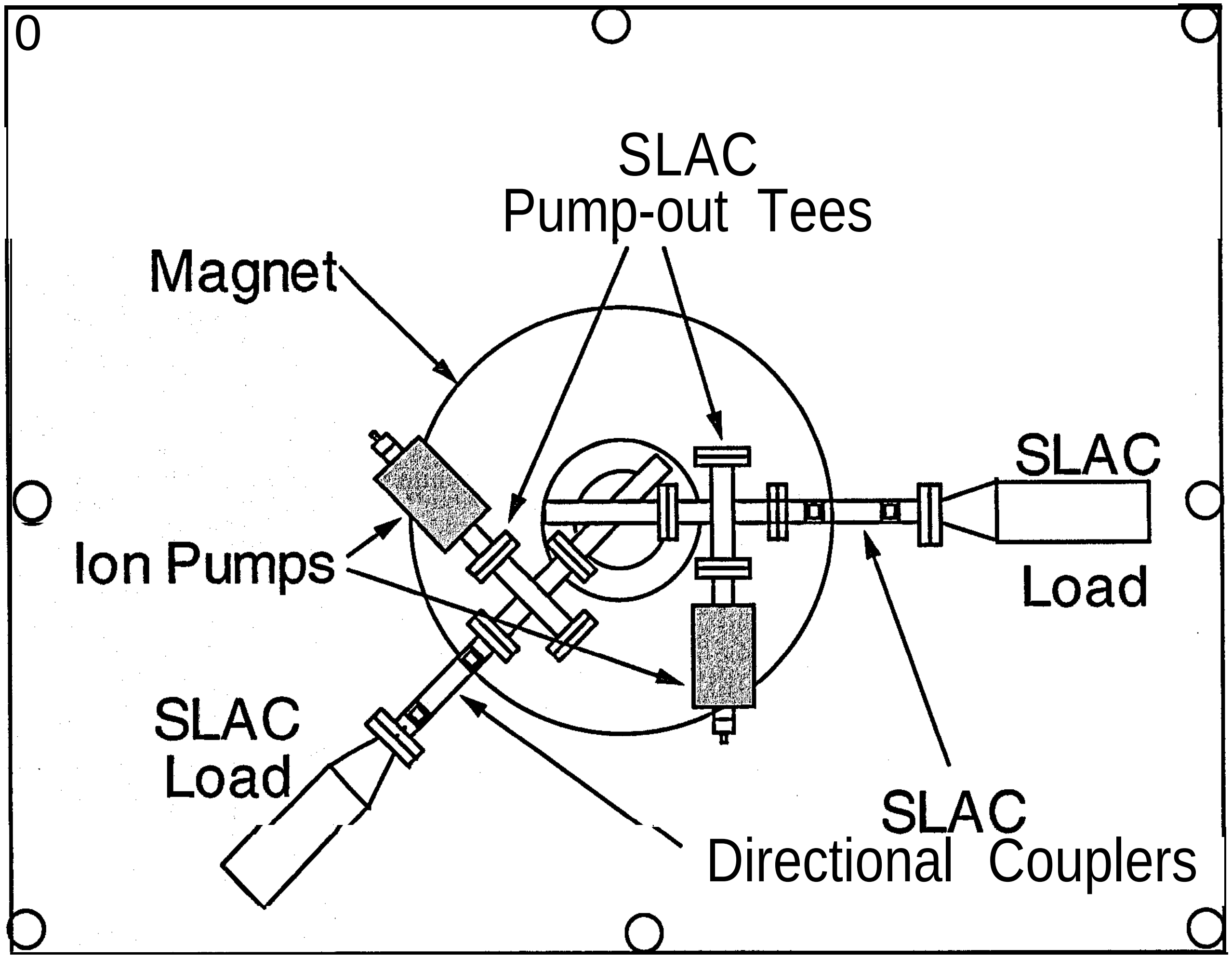

Figure 10. Schematic diagram of the magnicon rf output system

vacuum. However, the use of the 11.424–GHz radiation to power other experiments requires output windows. For the first experiment using the magnicon to drive a single–channel active microwave pulse compressor (see Section IV.C), we made use of an "old–style" SLAC TE_{11} window assembly on a single magnicon output arm. That window was donated to the magnicon program by Dr. Caryotakis of the Klystron Group at SLAC. At 1–μs pulse length, this window is rated at a maximum of 15 to 20 MW of peak power into a matched load, and perhaps only one–fourth of that power into a severely mismatched load such as a resonant cavity. (Under the new Interagency Agreement, high–power windows capable of transmitting the full magnicon power, even in the presence of severe load mismatch, will be acquired.)

Figure 11 shows a scale drawing of the magnicon experimental configuration, including the gun, magnet, cavities, and collector. The two output waveguides shown are standard SLAC double–wall–thickness WR–90 waveguide, using SLAC–style connecting flanges. Note that the two output waveguides are shown 180° apart, but are actually separated by 135°.

J. Diagnostics

In ordinary operation, there are eleven microwave signals displayed as oscilloscope traces. These are: drive signal, reflected signal from the drive cavity, signals from the three gain and two penultimate cavities, and forward and reflected signals from the directional couplers on each of the output arms. Each of the microwave signals is transmitted through a calibrated coaxial cable, reduced to a suitable level for detection by calibrated attenuators, and measured by calibrated crystal detectors. Also observed are the modulator current and voltage pulse, the collector current trace, and the collector button current. Thus, a total of 15 signal traces are monitored simultaneously on separate oscilloscope traces. In addition, the pressures in the five ion pumps are constantly observed. Also, the drive frequency is displayed by a frequency counter, the water flow through the high power loads is displayed by a flowmeter, the water

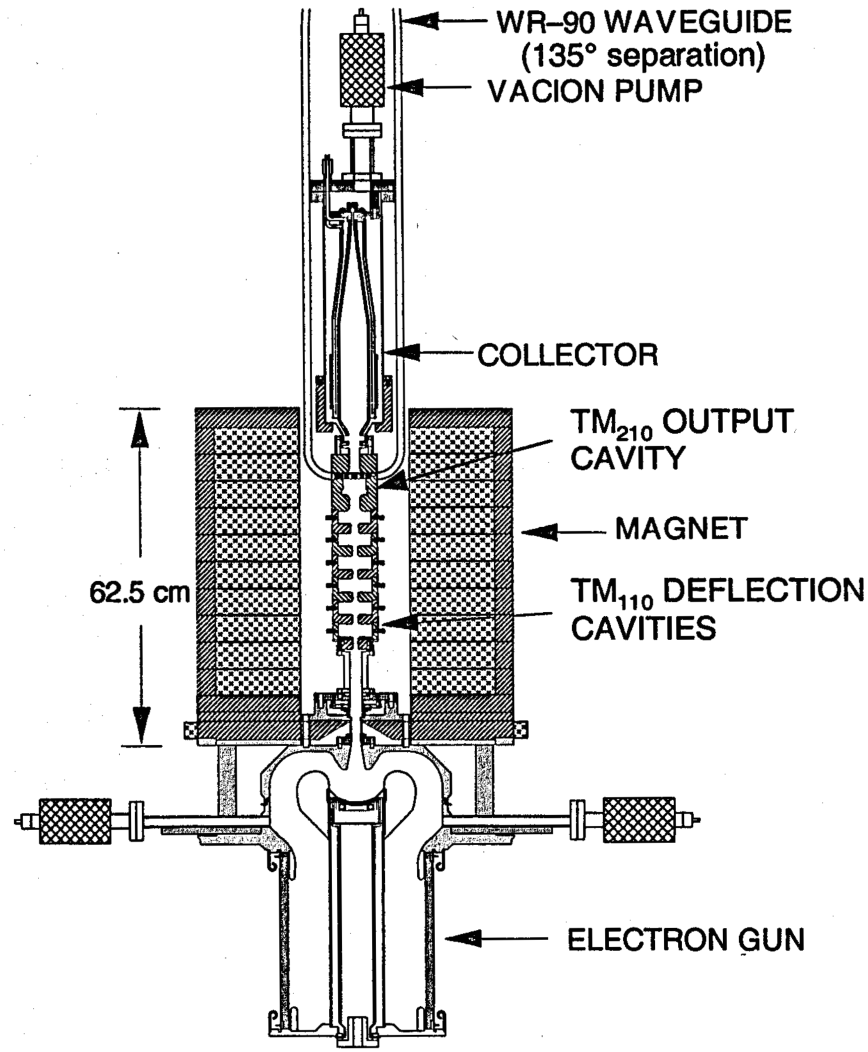

Figure 11. Scale drawing of the NRL X-band magnicon amplifier experiment

temperature at the input and output of the calorimetry setup, as well as ΔT, are displayed, digital readouts show the current in the ten magnet coils (four separate variable power supplies) and in the bucking coil, and digital readouts also show the modulator control parameters, including repetition rate (pulses per second), PFN charge voltage, and gun heater current and voltage.

The most certain diagnostic of microwave power is calorimetry, i.e., detecting the temperature change caused by microwave energy deposition into a matched rf load. Unlike ordinary microwave diagnostics, which employ many tens of dB of calibrated attenuation following by crystal detectors that measure output signals at the mW power level, calorimetry provides a direct and reliable measurement of average output power. For this reason, a calorimetry setup was put in place on the output of the 11.424–GHz magnicon. A block diagram of the experimental calorimetry setup is shown in Fig. 12. The end of each output waveguide arm is a SLAC low–average–power "dry" load [14]. These loads absorb the microwave energy in a set of lossy stainless–steel cavities. The exterior of each load is wrapped with a metal water pipe that allows for load cooling. This becomes a calorimetry diagnostic when the water jackets of the two loads are connected in series, the loads are thermally isolated, the water flow rate is monitored, and the change in water temperature is monitored while pulsing the magnicon in a reproducible, rep–rated set of experimental conditions. The water flow is measured by a conventional sight–glass flow–meter and by a Ryton 50–500 mL/min flow sensor with a digital read–out. The flow sensor was calibrated against the timed flow of water into a graduated cylinder. The temperature change is read out using a Digi–Sense Dual Thermocouple Thermometer, which reads out ΔT directly to a precision of 0.1° C. In order to provide the necessary thermal isolation, the two loads were placed in separate wooden boxes lined with plastic foam insulation, and the water line linking the loads is also surrounded by plastic foam pipe insulation. In steady state, the product of water flow, water heat capacity, and temperature change is an absolute measure of the average power deposited in the loads. If the average power

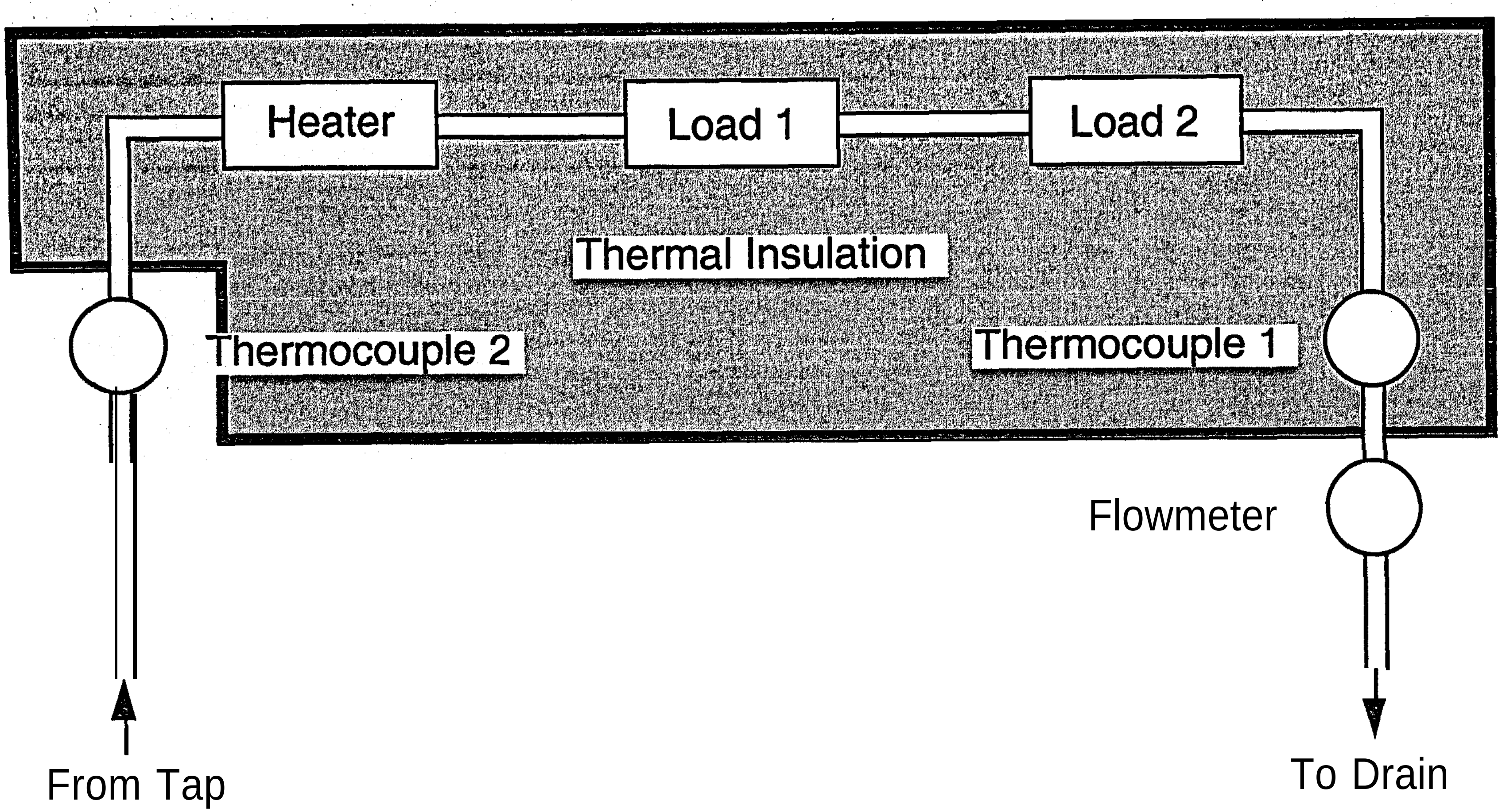

Figure 12. Block diagram of calorimetry system

is divided by the product of output pulse length and repetition rate, the average power in the output pulse can be determined. However, to correct for real–world thermal losses, which can reduce the measured power below its true value, a thermal calibration setup was also used, consisting of a water heater in line with the first of the two loads, and within the thermal insulation jacket. The water heater is powered by a Variac, in order to make possible the controlled addition of a known amount of power into the flowing water.

Determination of the spectral content and phase stability of the output requires heterodyne measurements. Figure 13 shows a block diagram of the basic setup for these measurements. To measure the spectral content, the signal from one of the two output directional couplers is combined with a signal from a separate tunable local oscillator (HP8690B Sweep Oscillator with H40–8694A 7–12 GHz plug–in) in an Anzac MDC–182 double–balanced mixer. The mixer output is sent to a Tektronix DSA602 1–GHz analog bandwidth, 2 GS/s digital storage oscilloscope, with a built–in fast–Fourier–transform (FFT) function. With this setup, output frequency components within ±1 GHz of the local oscillator frequency can be observed and measured, subject to an uncertainty in the sign of Δf. The latter uncertainty is resolved by tuning the local oscillator, and observing whether a particular peak moves to lower or higher frequencies. This same diagnostic was used to measure the output phase stability (see Section IV.B), a key requirement for accelerator applications, by using the second harmonic of the drive signal as the local oscillator.

K. Simulation of the Magnicon Experiment

Figures 14 and 15 show time–dependent and steady–state simulations of magnicon operation. These simulations were carried out with the fully 3–dimensional magnicon simulation code [15,16] using the measured parameters of the electron beam. The beam parameters employed, and the resulting magnicon parameters, are shown Table I.

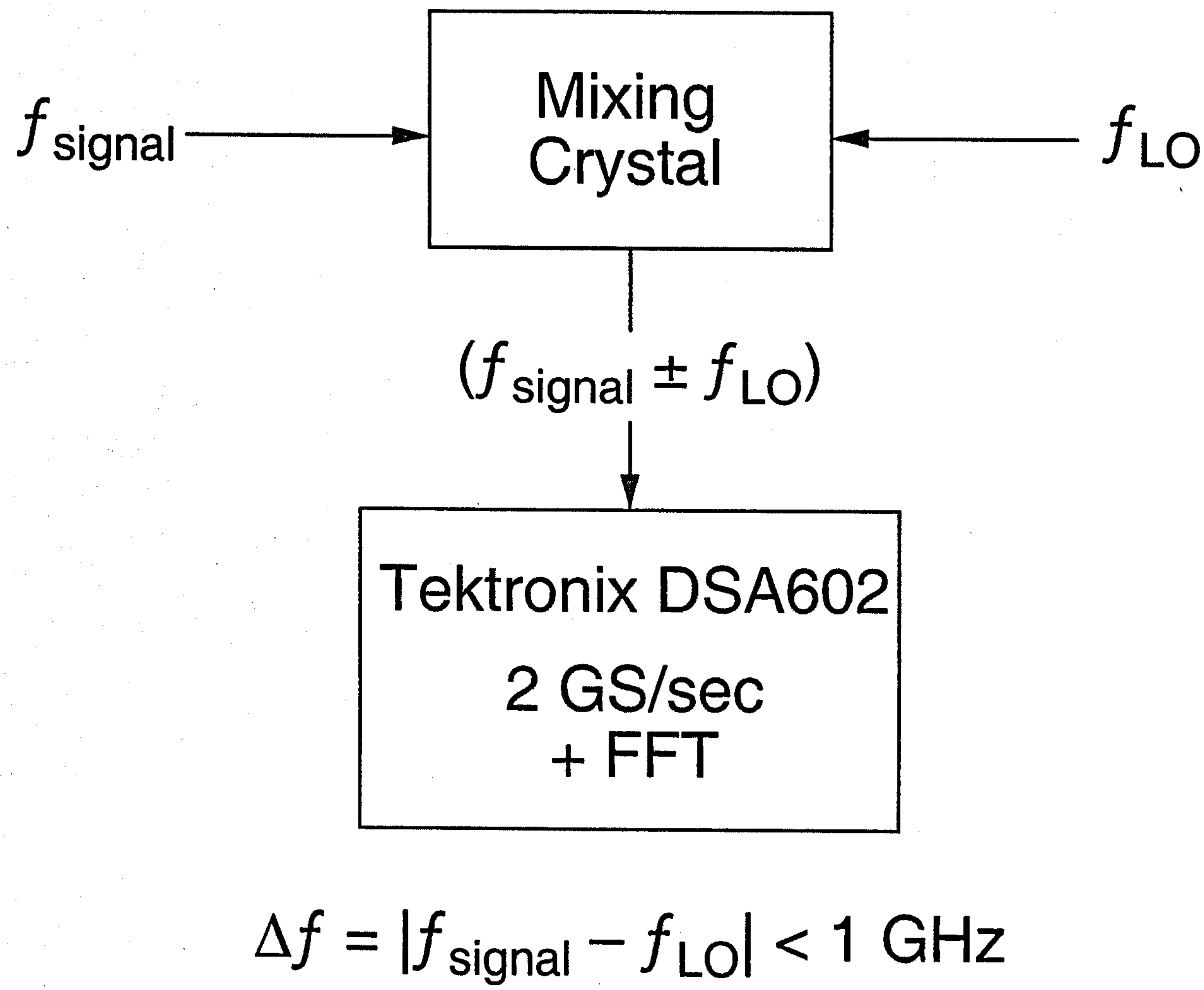

Figure 13. Block diagram of heterodyne frequency diagnostic

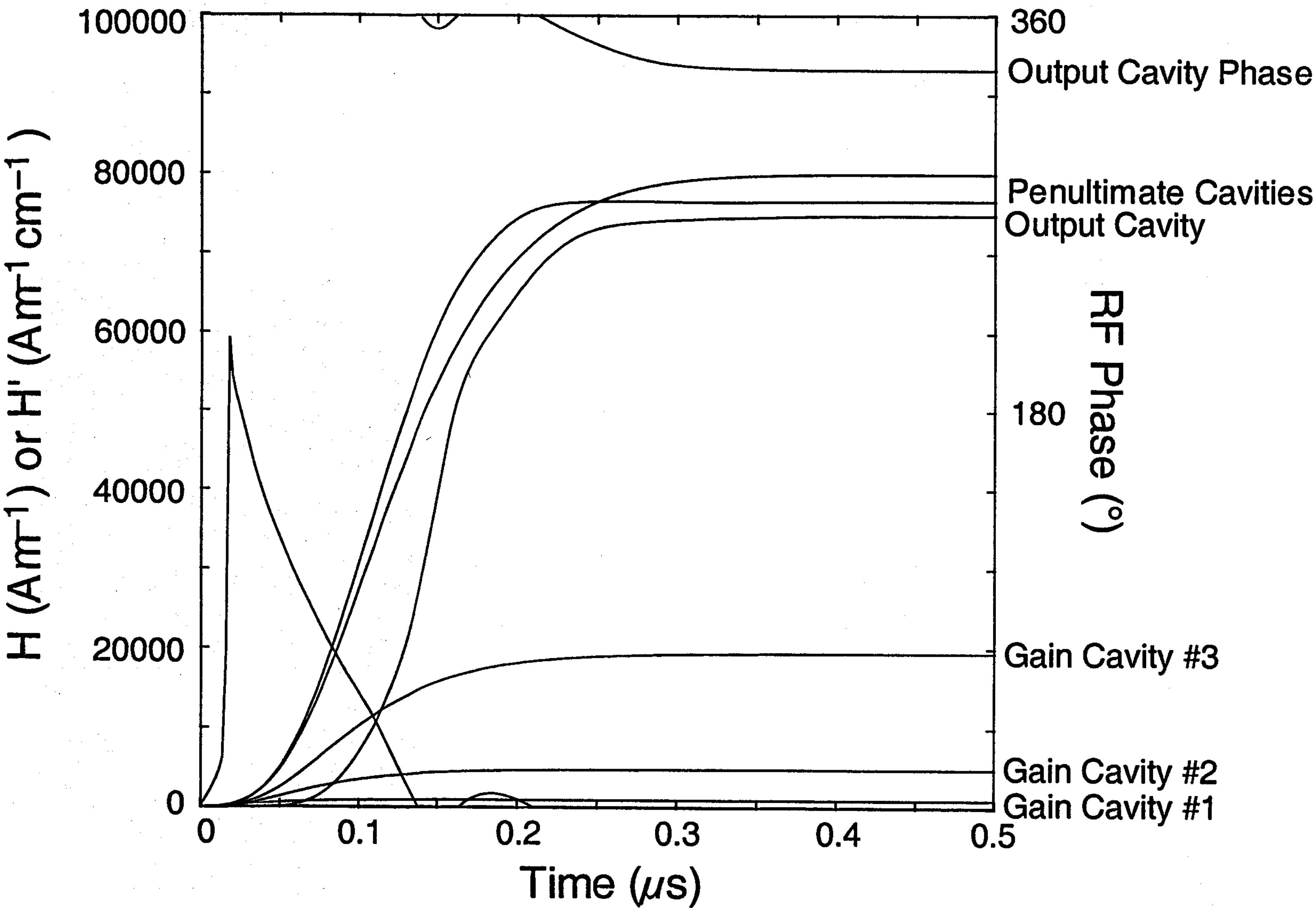

Figure 14. Time-dependent simulation of magnicon operation

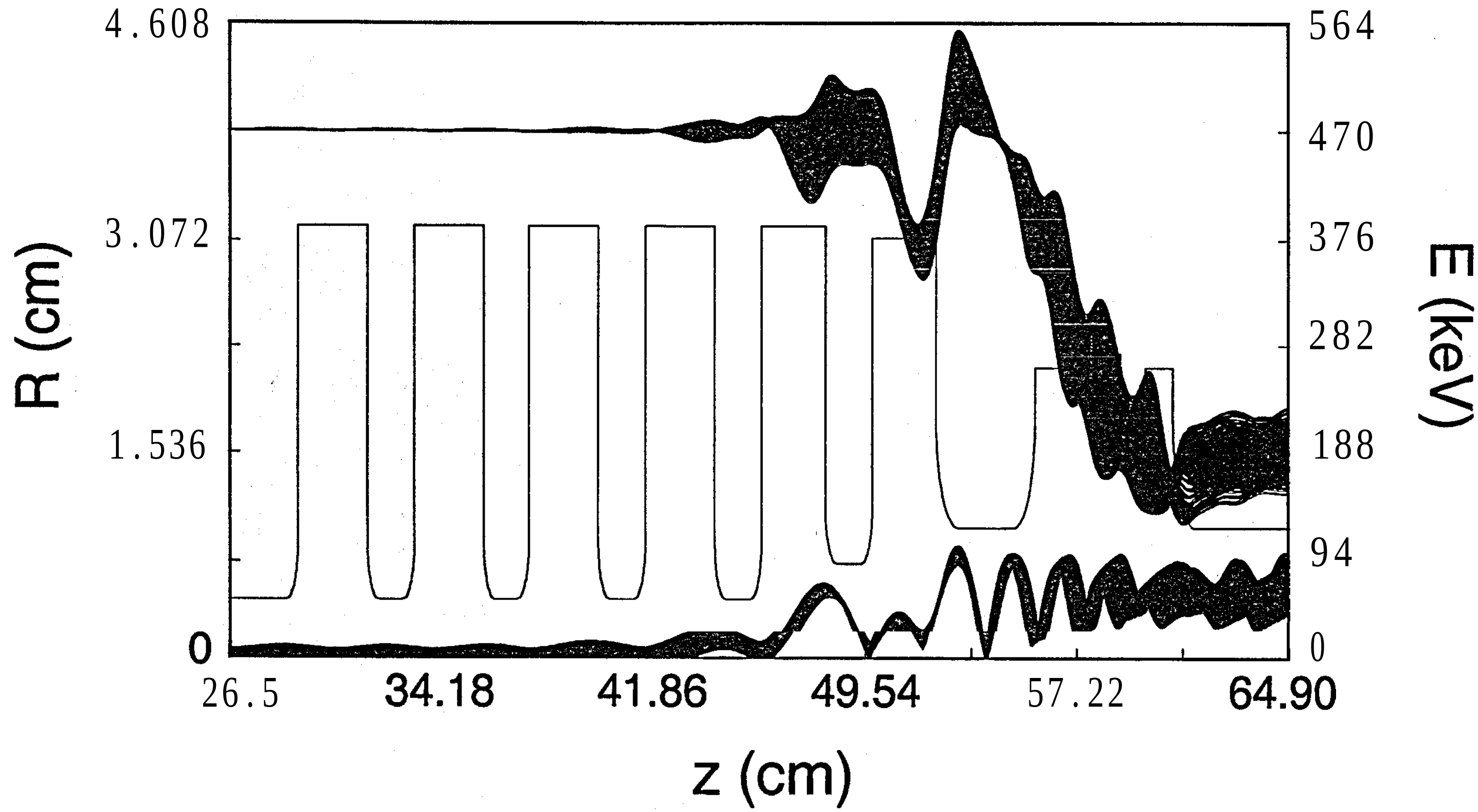

Figure 15. Steady-state simulation of magnicon operation

Table I. Magnicon Design Parameters

Beam voltage	470 kV
Beam current	220 A
Beam radius (mean)	0.93 mm
Input Power	80 W
Output Power	61 MW
Gain	59 dB
Efficiency	59%
Maximum pulse length	~1.1 μs
Maximum repetition rate	10 Hz

IV. Experimental Results

A. Introduction

Initial operation of the reassembled magnicon experiment took place on 21 November 2000, following completion of beam measurements on the rebuilt electron gun. The turn–on of any high–power tube requires an extended period of rf–conditioning before full–power operation can take place. This process had not been completed by the end of the Agreement. In this Section, we summarize the operating performance of the magnicon as of 15 May 2001 and also discuss the results of the first use of the magnicon as a high–power source to test an active microwave pulse compressor. Figure 16 shows a photograph of the magnicon experimental setup.

B. Magnicon Results

Magnicon conditioning was carried out through February 2001. At the end of February, before the conditioning was complete, the magnicon circuit was brought up to 1 atmosphere of dry nitrogen, with the gate valve closed, for installation of an output window. Tests of an active pulse compressor, as described in the next section, were carried out through March and April 2001. At the conclusion of this period, the circuit was again brought up to dry nitrogen for removal of the output window, to permit high–power conditioning to resume. By 15 May, conditioning was again under way, but the results of February 2001 had not yet been surpassed. In this section, we describe the magnicon results that were produced in January and February 2001, following several months of conditioning.

Figure 17 shows a set of traces from the two magnicon output channels and the result of simultaneous calorimetry measurements. These traces correspond to the maximum output power of ~15 MW observed at the maximum available pulse width with no pulse shortening

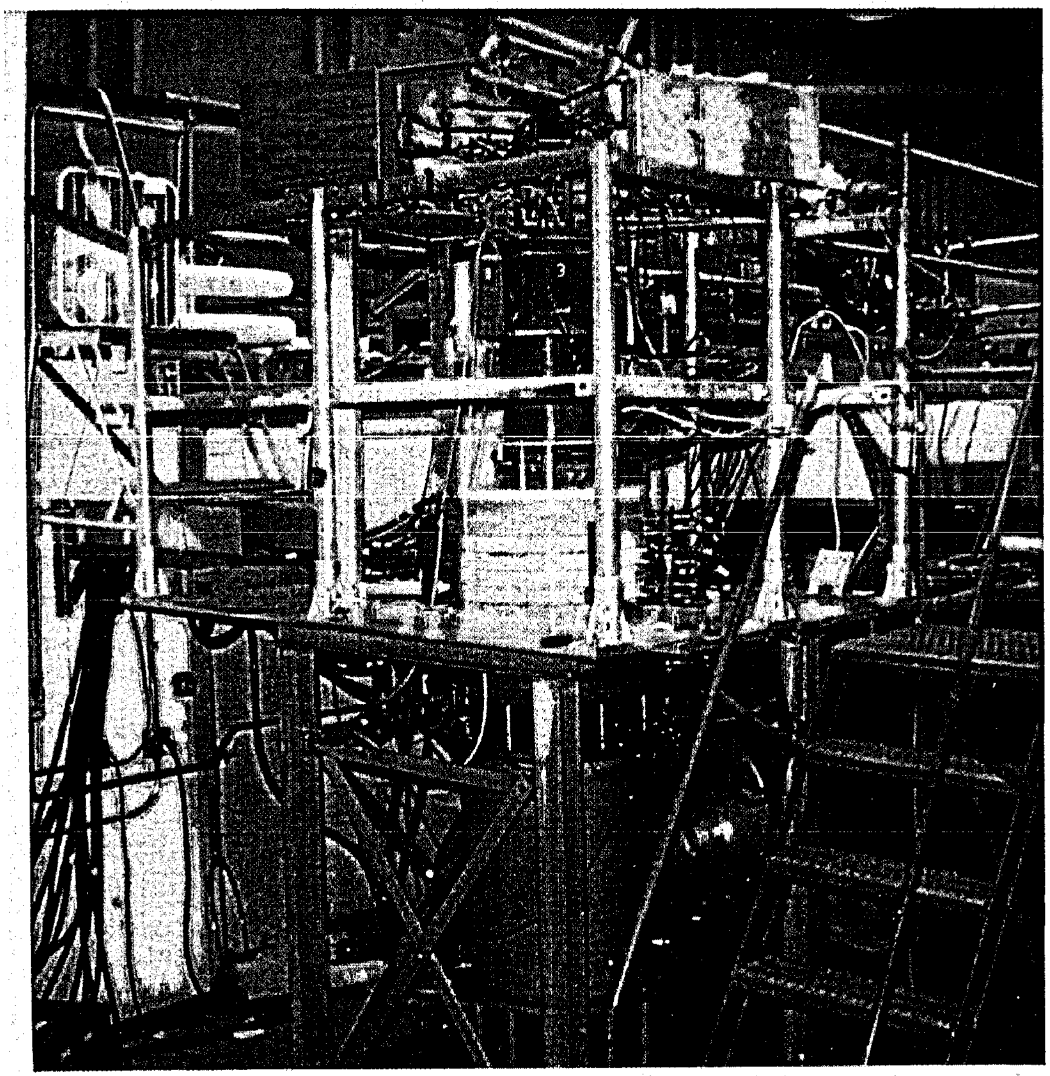

Figure 16. photograph of 11.424-GHz magnicon

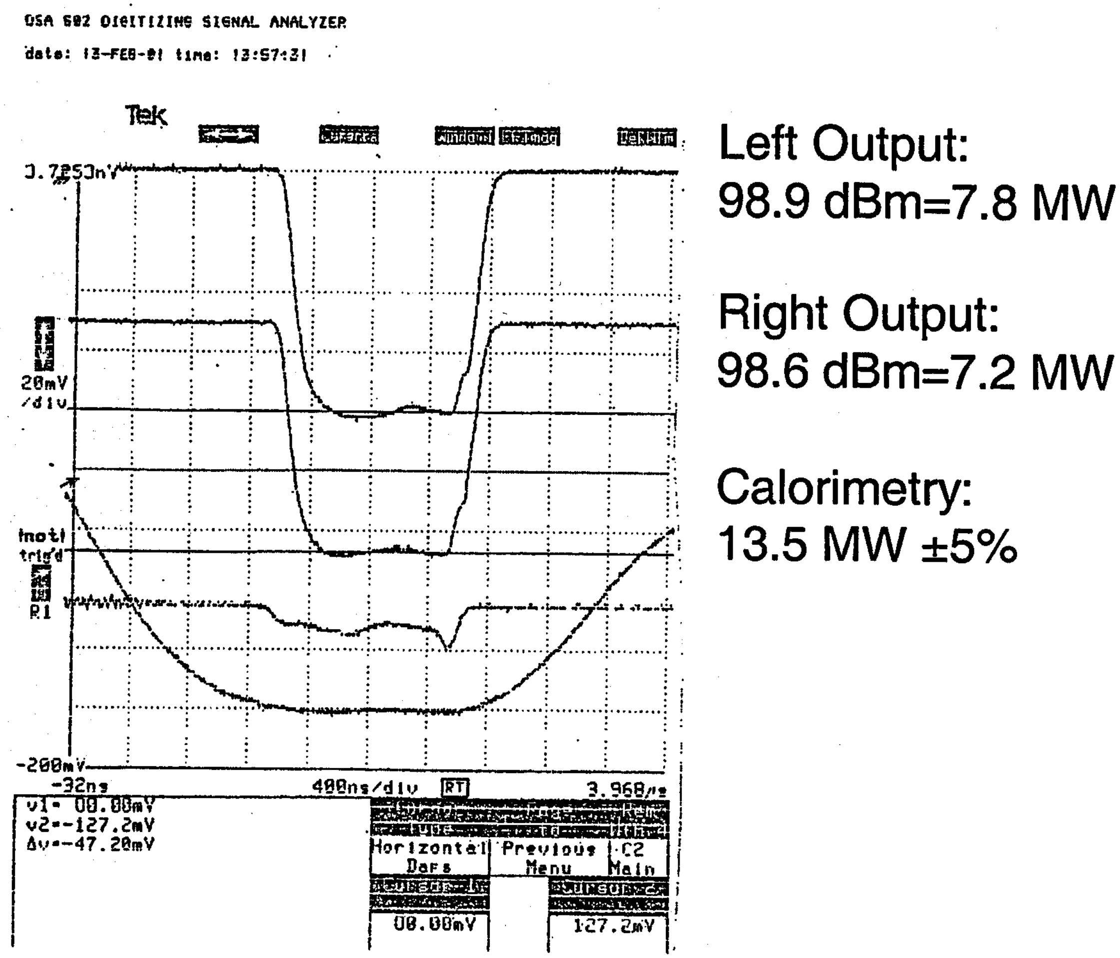

Figure 17. Magnicon output waveforms corresponding to 15 MW, 1.2 μs operation

effects apparent. The calorimetry required that the operating conditions remain unchanged for at least 30 minutes because of the thermal inertia of the calorimeter. The data was taken at a repetition rate of 2 Hz. The left and right output waveguides show very similar signal levels, 7.8 MW and 7.2 MW respectively, with the small apparent asymmetry of 0.3 dB within the relative calibration error. Based on the duty factor, the calorimetry showed a power of 13.5 MW with a 5% uncertainty. The FWHM of the microwave signal in this case was 1.2 μs. The operating conditions were 430 kV and ~200 A with a 5.7129 GHz drive frequency.

The maximum output power could be increased at shorter pulse lengths. Figure 18 shows two sets of traces demonstrating ~20 MW in a 440 ns pulse and ~25 MW in a 220 ns pulse. (In the second case, a parasitic oscillation is visible at the end of the output pulse.) By using short drive pulses, these higher power signals were produced without pulse shortening.

Figure 19 shows a magnicon drive curve, i.e., power out versus power in under constant experimental conditions (frequency, current, voltage, and magnetic field). A smooth, well–behaved drive curve is apparent, indicating that in this regime the tube essentially operates as a linear amplifier. The magnicon output was analyzed with a shorted, slotted line, and no evidence of parasitic oscillations were found. Figure 20 shows the output power versus drive frequency for constant drive power and constant experimental conditions. The FWHM is the curve is ~4 MHz, corresponding to a bandwidth of ~.07%. (It is important to note that this bandwidth may change when the conditioning is complete.)

One important test of an amplifier is the phase stability of the output. Figure 21 shows the experimental setup for a test of the phase stability of the magnicon. A double–balanced mixer is used to combine an output signal from one of the two waveguide arms with the drive signal. Because of its nonlinearity, the mixer also generates harmonics of the drive signal. Since the output bandwidth is <500 MHz, only low frequency components of the combined signal can be detected. In particular, the output is sensitive to $E_{drive}E_{out}\cos[(2\omega_{drive}-\omega_{out})t-\phi]$, as

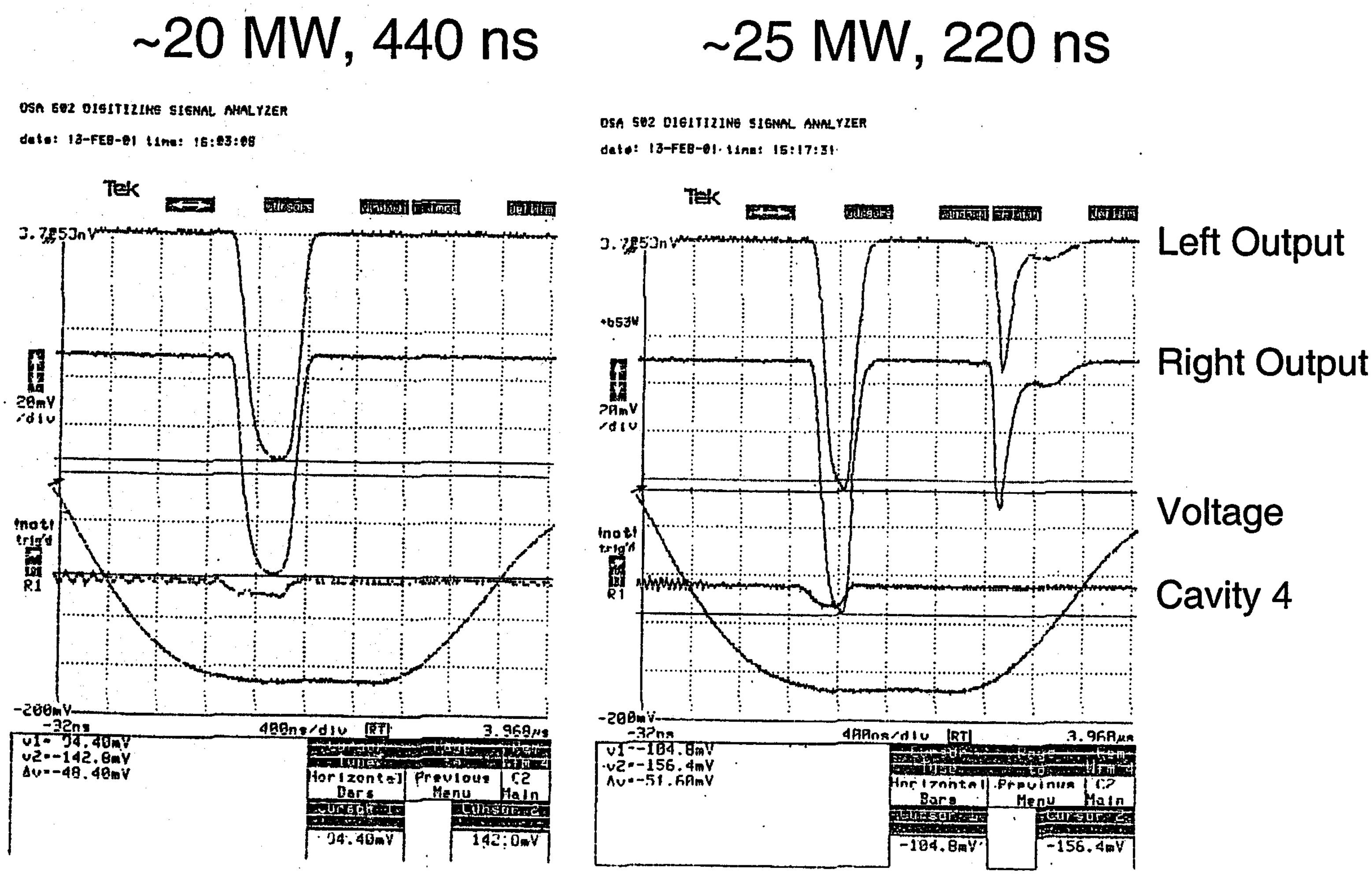

Figure 18. Magnicon output waveforms corresponding to high power, short pulse operation

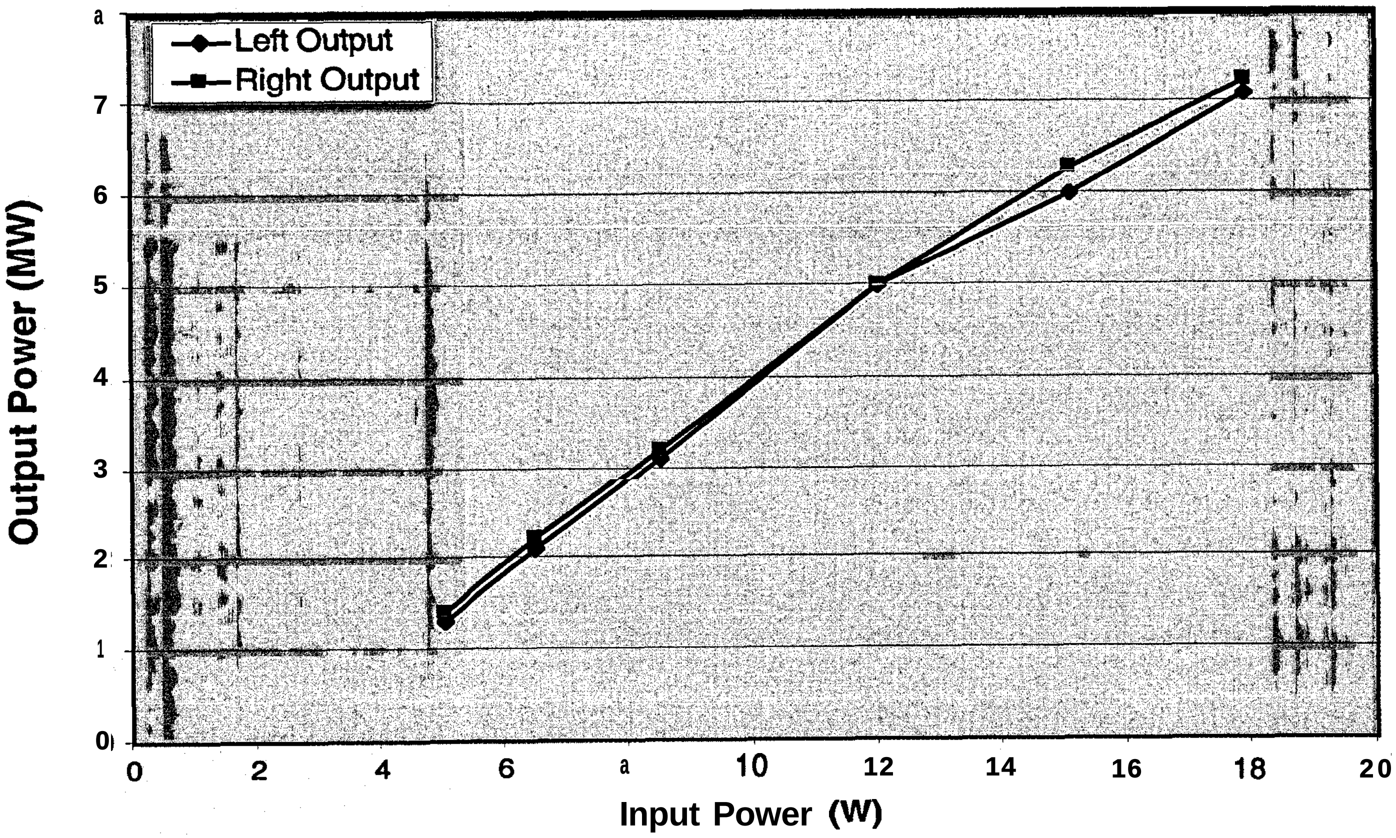

Figure 19. Magnicon drive curve at 5.712 GHz

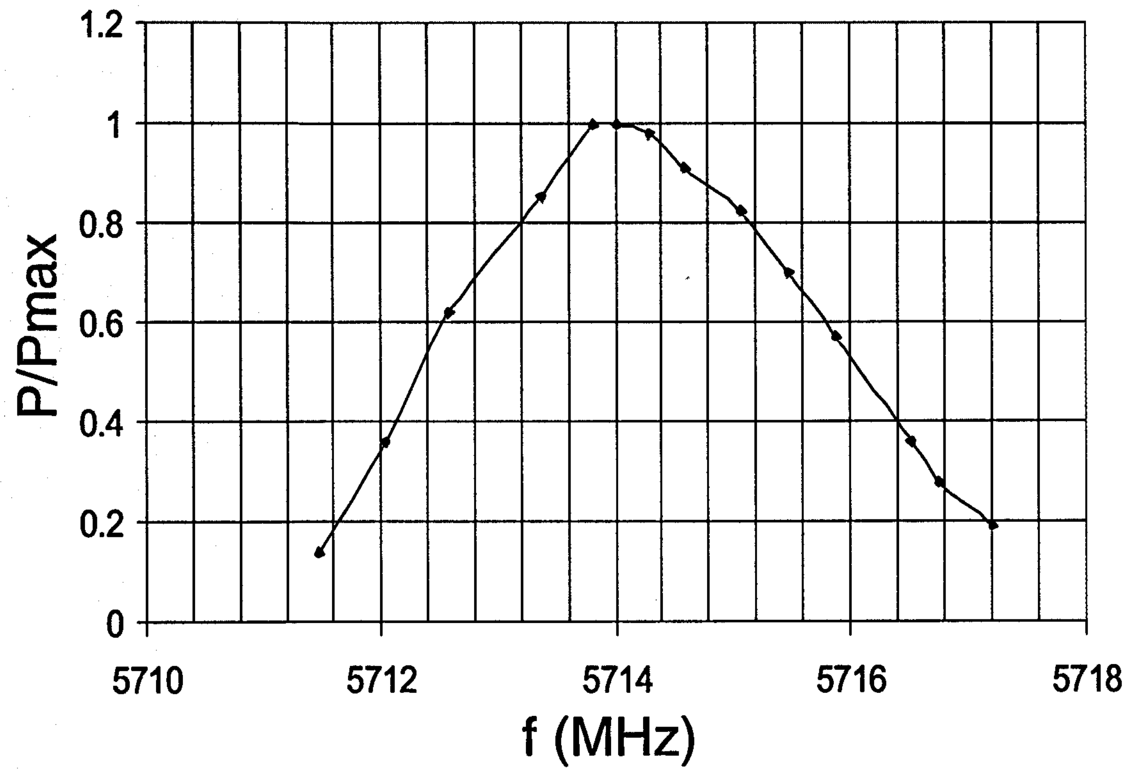

Figure 20. Magnicon output power versus drive frequency

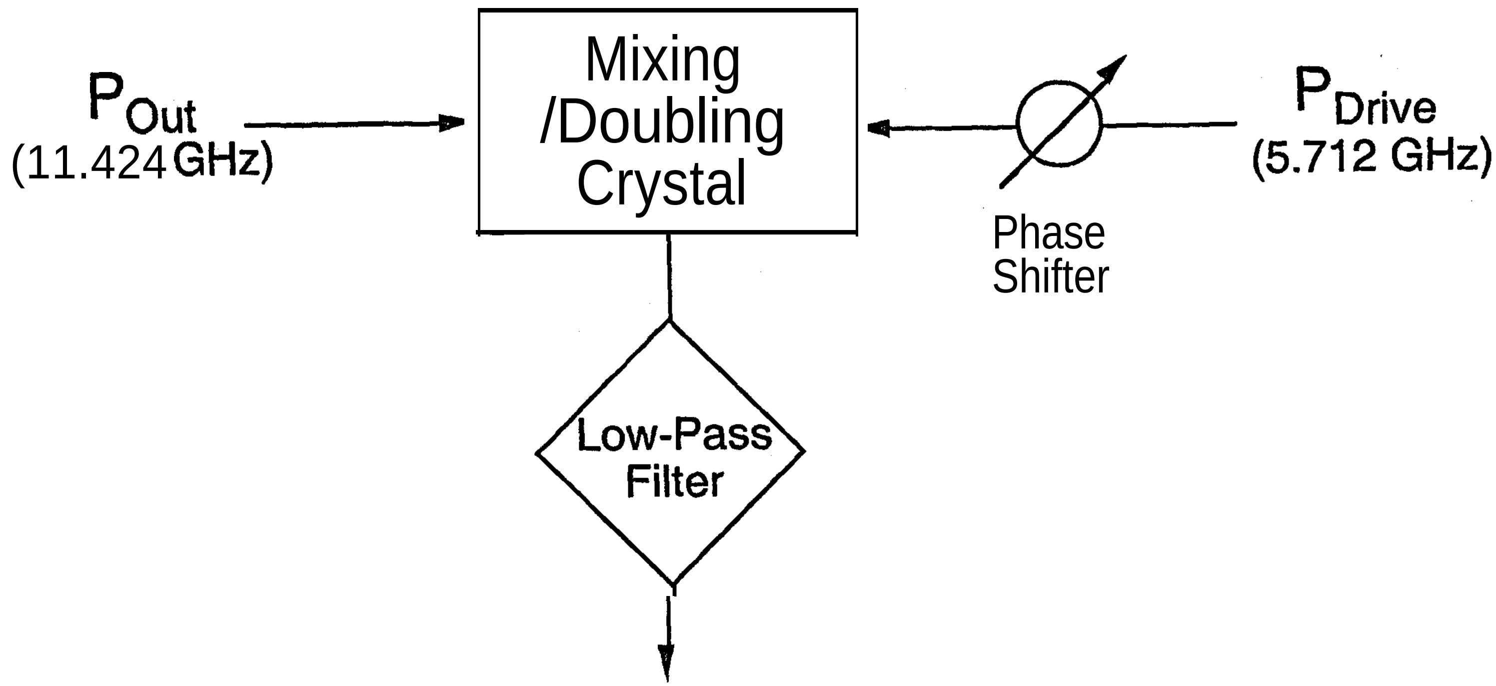

$$V \propto -\left[E_O^2 + E_D^2 + \alpha E_O E_D \cos[(2\omega_D - \omega_O)t - \phi] \right]^{1/2}$$

Figure 2 1. Block diagram of output phase diagnostic indicated in the figure, where ϕ is a phase factor. A phase shifter in the drive line allows ϕ to be varied. Figure 22 shows the results of a phase stability measurement. Data were taken for three settings of the phase shifter shown in Fig. 21. The phase–shifter settings were chosen to produce a maximum of the beat signal, a minimum of the beat signal, and finally a signal half–way between the maximum and minimum. The third setting is best for determining the flatness of the phase during the voltage "flattop." The third set of traces demonstrates a phase variation of approximately $\pm 10°$ due to the voltage ripple. However, there is no noticeable change in the shot–to–shot phase at a single setting of the phase shifter, indicating that the output is phase is locked to the phase of the drive signal.

C. Tests of an Active Pulse Compressor

During March and April 2001, the output from a single arm of the magnicon was extracted through an output window into an active microwave pulse compressor called an Active Bragg Compressor (ABC) [8]. Figure 23 shows a simple schematic of the ABC, along with its design parameters. The ABC makes use of an electrically–triggered gas–filled quartz switch tube to shift the resonant frequency of a cavity end reflector, thus changing the compressor from a high–Q state for energy storage to a low–Q state for energy extraction. Low–power tests of this system at NRL had already demonstrated an rf power multiplication of 11–12×, with an output pulse length of ~50 ns FWHM. These high–power tests were intended to determine the switching time, energy efficiency, power limitation, and lifetime of the switches, but not to produce flat–topped output pulses. (Creation of flat–topped pulses can be achieved by installing plasma switches on a SLED–II structure.) These tests were made in collaboration with Dr. Anatoly Vikharev and coworkers from the Institute of Applied Physics in Nizhny–Novgorod, Russia, who developed the ABC. Their work was carried out under the auspices of a DoE SBIR contract with Omega–P, Inc. Figure 24 shows a photograph of the ABC on its

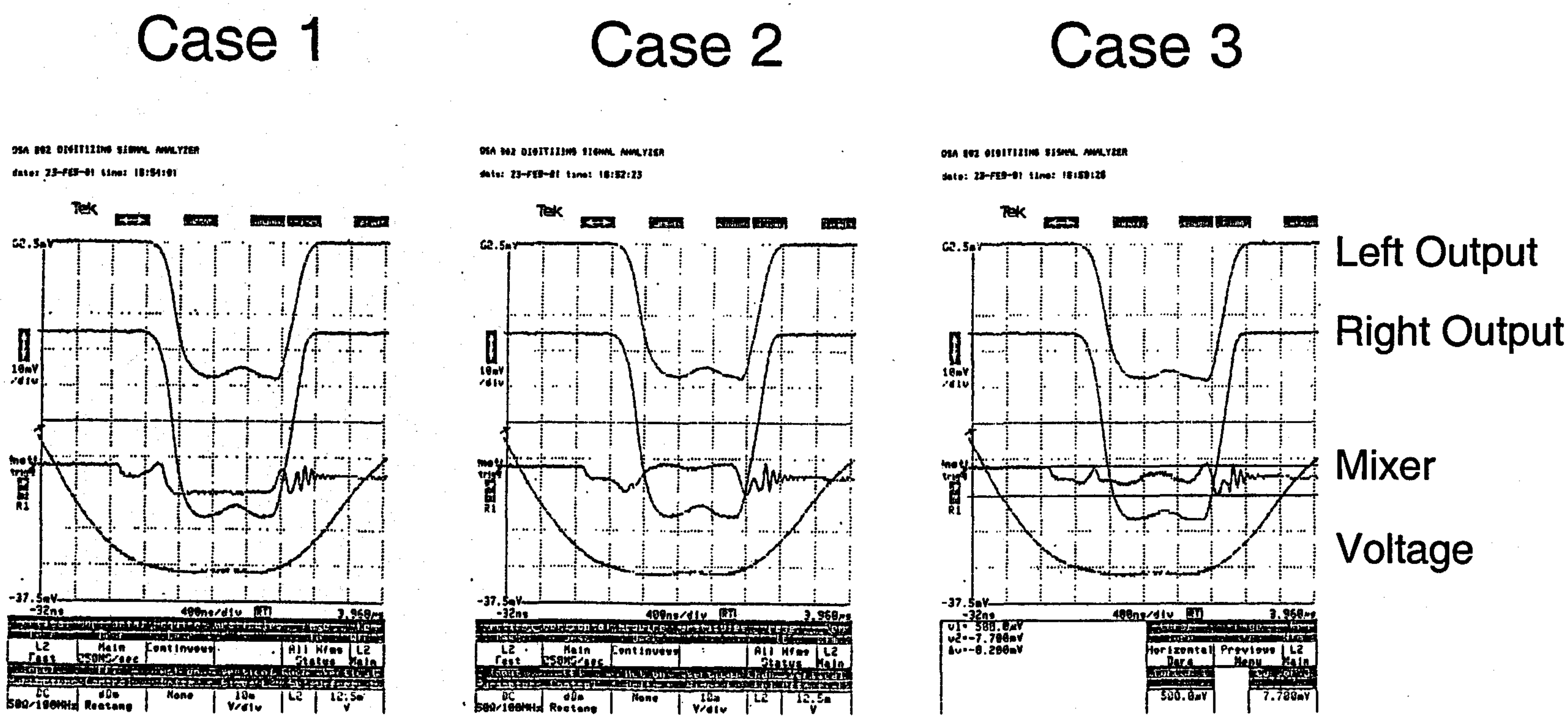

Figure 22. Magnicon output waveforms for phase stability measurements. The mixer signal is the phase sensitive product of the output signal and the second harmonic of the input signal. The 3 cases correspond to different adjustments of the phase shifter on the input signal.

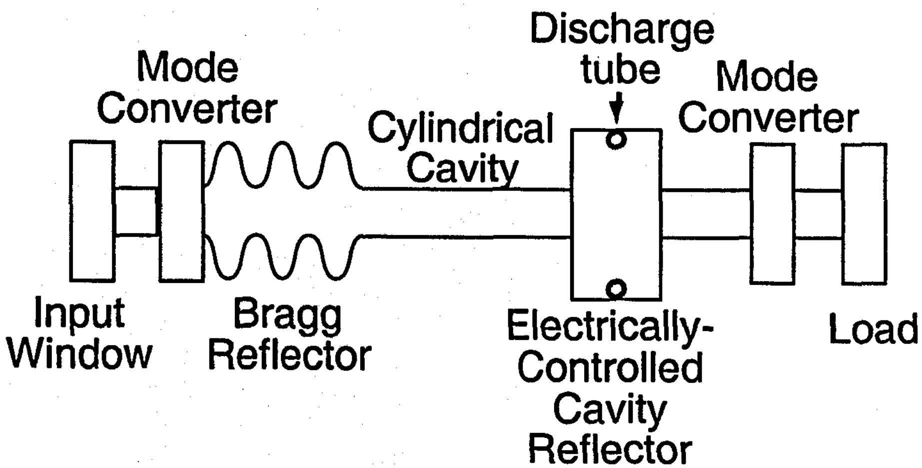

<u>Design Parameters</u>

Input Power	10-30 MW
Input Pulse Length	1 μsec
Compression Ratio	10-12
Output Pulse Length	80 nsec
Output Power	>100 MW
Efficiency	60%

Figure 23. Schematic of Active Bragg Compressor, with design parameters

platform in the NRL Magnicon Facility, and Fig. 25 shows a photograph of the ABC connected to one output arm of the magnicon. The waveguide window region is shown covered with aluminum foil for a bakeout procedure.

During the ABC tests, it was necessary to condition both the output window and the switch region of the ABC. It was observed that at high power, the ABC would self–switch due to breakdown on the exterior of the quartz switch tube. The threshold for this process gradually increased as conditioning progressed. However, it never approached the 10 MW level called for in the design. Also, it was observed that the magnicon output was affected by the pulse compressor, which constitute a resonant load. The normally flat magnicon output waveform became time dependent. This is clearly visible in Fig. 26, which shows incident, reflected, and output waveforms from a test of the ABC in the self–break regime. The magnicon output (from a single arm) reaches a maximum of 4.2 MW early in the cavity fill–time, when the cavity is strongly mismatched, and decreases to less than half that value later in the fill–time, when the cavity is a better–matched load. The self–switching produces a 14.5 MW, 50–60 ns compressed output pulse from a ~1.2 μs drive pulse with an average power ~2.3 MW, for a power gain of ~6.3. By backing off on the drive power to below the self–switch threshold, active switching of the ABC could be demonstrated. Figure 27 shows a test of the ABC in the triggered mode. In this case, an average incident power of ~0.7 MW is compressed into a 4.5 MW, 60–70 ns output pulse.

These first high–power tests of the ABC showed a serious problem with multipactor breakdown on the exterior of the quartz switch tubes. As a result, the switch region is being redesigned by Vikharev and coworkers at the IAP to reduce the rf fields in the vicinity of the quartz tube. In addition, a low–secondary–coefficient TiN coating will be applied to the quartz tube to suppress multipactor breakdown.

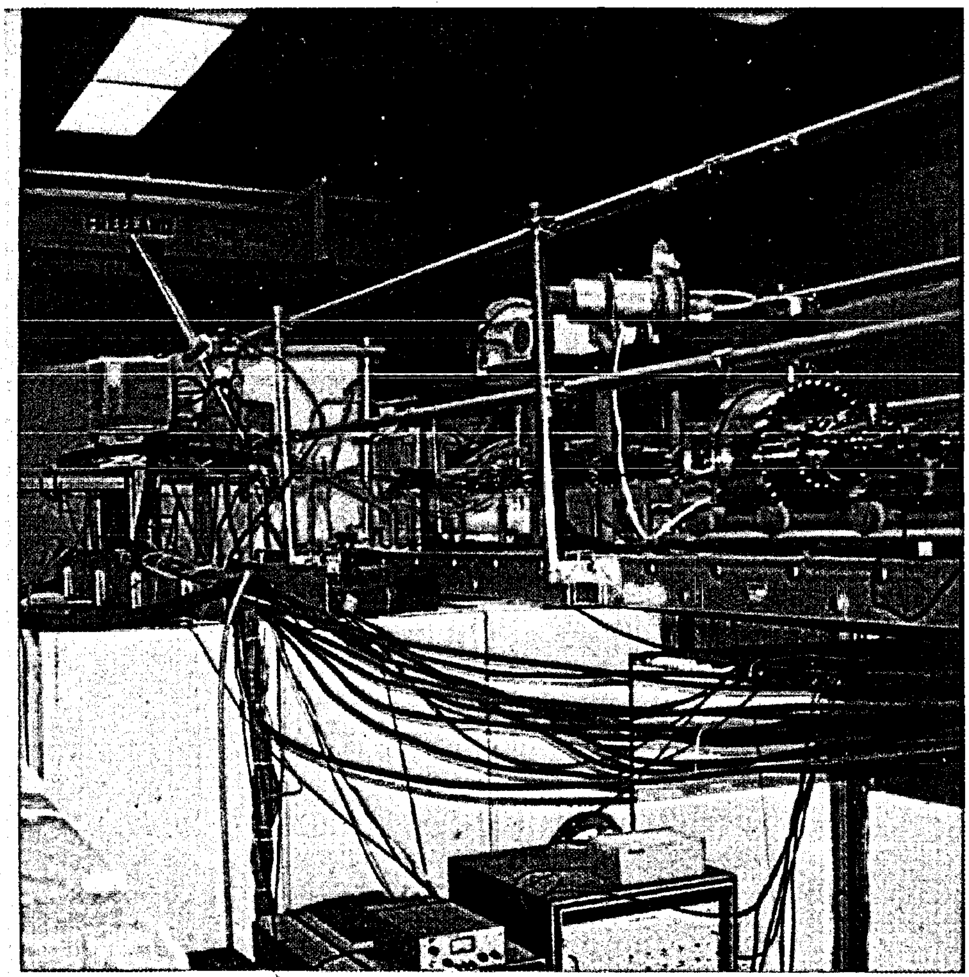

Figure 24. Photograph of 11.424-GHz Active Bragg Compressor in NRL Magnicon Facility

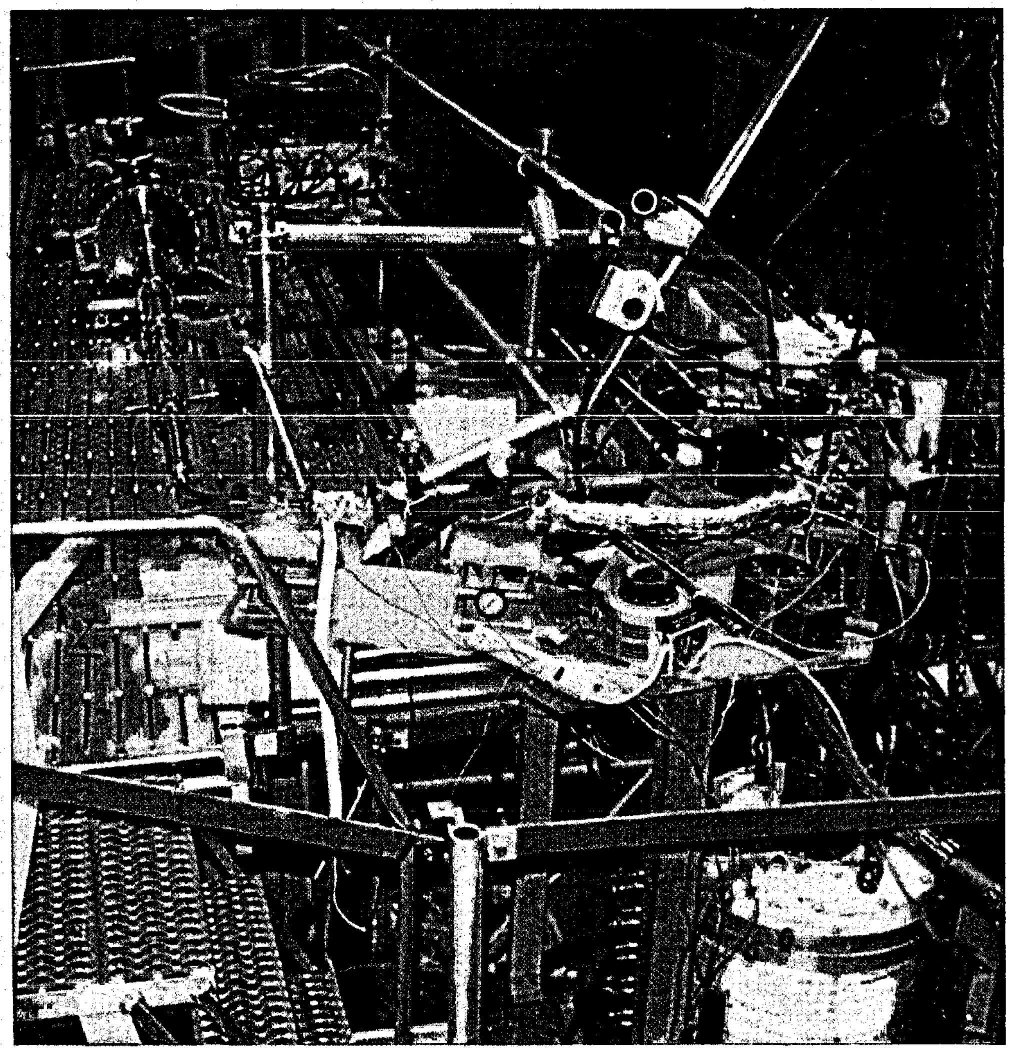

Figure 25. Photograph of **11.424-GHz** Active Bragg Compressor coupled to magnicon output

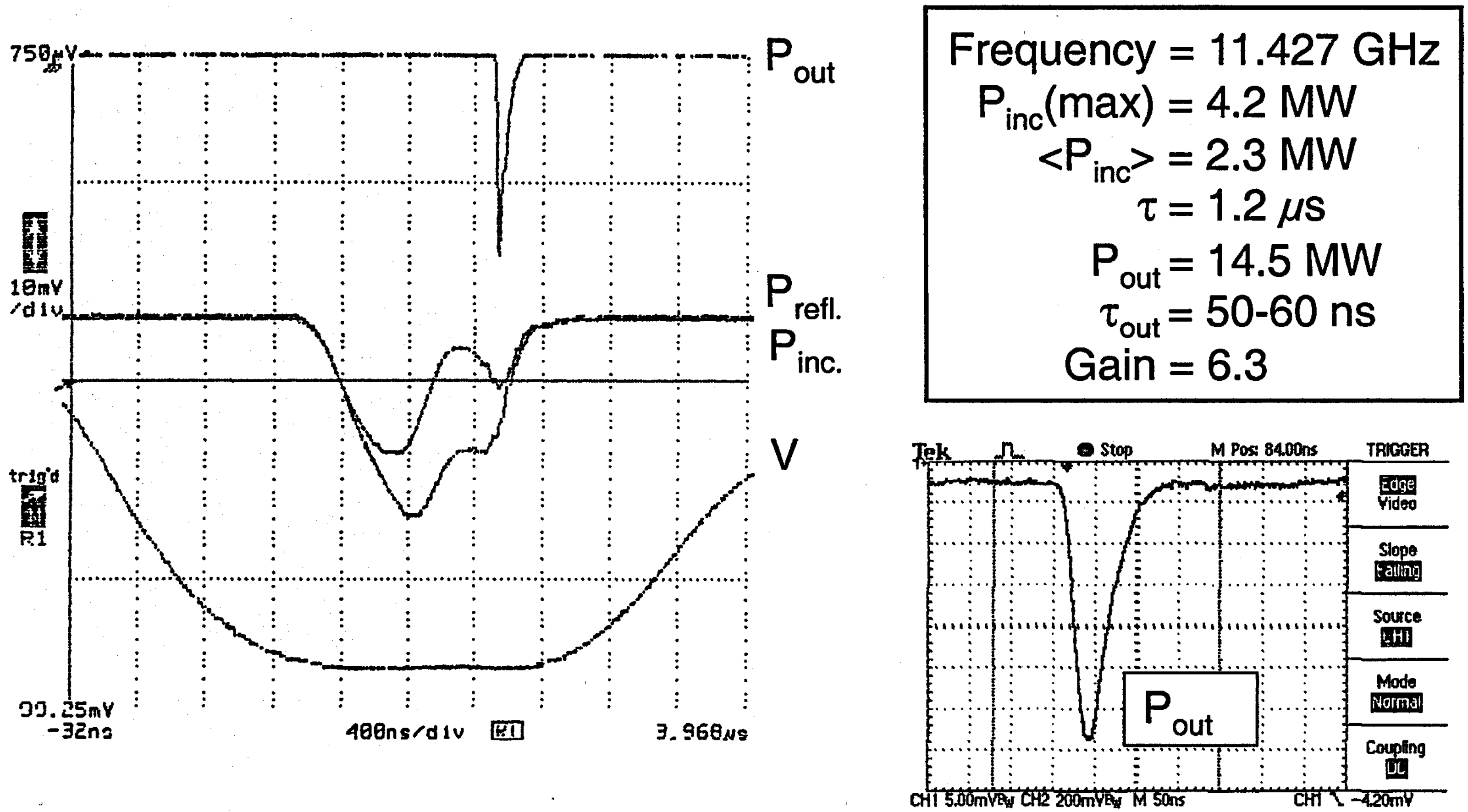

Figure 26. Pulse compressor traces—non-triggered mode

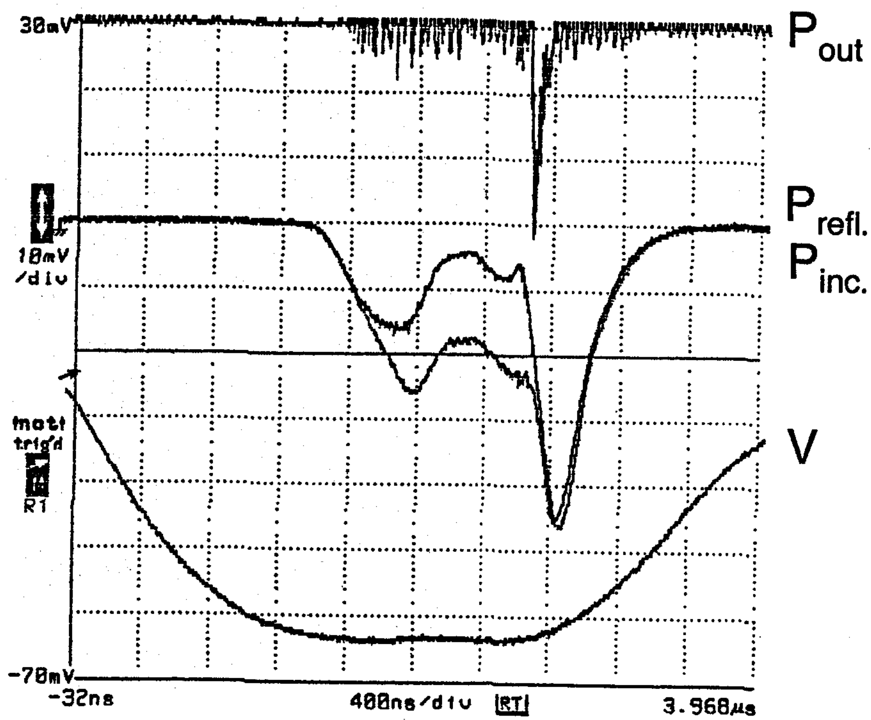

Frequency = 11.427 GHz
P_{inc}(max) = 1.2 MW
$\langle P_{inc} \rangle$ = 0.7 MW
τ = 1.2 μs
P_{out} = 4.5 MW
τ_{out} = 60-70 ns
Gain = 6.4

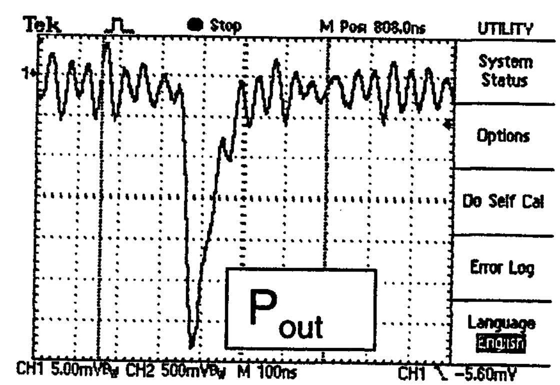

Figure 27. Pulse compressor traces—triggered mode

V. Summary

At the conclusion of this Interagency Agreement (15 May 2001), the magnicon was undergoing its final high–power conditioning, having already demonstrated high–power operation (15 MW in a 1.2–μs FWHM pulse, 25 MW in a 200–ns FWHM pulse), phase stability, a well–behaved linear drive curve, a small operational frequency bandwidth, and a spectrally pure, single–mode output. In addition, the magnicon had already been used to carry out the first high–power tests of an active microwave pulse compressor in collaboration with Omega–P, Inc. and the Institute of Applied Physics (IAP) in Nizhny–Novgorod, Russia. In addition to testing the pulse compressor, these tests also demonstrated the ability of the magnicon to drive a resonant load. However, with the conditioning of the magnicon cavities not yet completed, the full magnicon design power level of >50 MW had not yet been achieved because of rf discharge effects in the cavities. The rf conditioning had produced steadily increasing output power levels, and it is believed that further conditioning will permit operation at the full design level. However, even at the level of output already demonstrated, the magnicon can be used to carry out tests of high–power structures and systems designed to operate at 11.424 GHz.

Based in part on these experimental results, the Department of Energy agreed to fund a new follow–on program, under a separate Interagency Agreement, to use the magnicon output to develop dielectric–loaded accelerators, in collaboration with the Argonne National Laboratory (ANL) and the Stanford Linear Accelerator Center (SLAC), and to develop active microwave pulse compressors, in collaboration with Omega–P, Inc. and the IAP.

Inverse Cerenkov accelerators using dielectric liners are a potential replacement for copper traveling–wave cavity structures, offering both a simpler smooth–walled geometry and reduced susceptibility to beam–breakup instabilities. However, the sustainable E–field gradients on dielectric walls at 11.424 GHz is presently unknown and requires experimental determination. Studies of traveling–wave and standing–wave dielectric–loaded accelerating structures will be carried out on the NRL Magnicon Facility under the new Agreement in collaboration with Dr. Wei Gai and coworkers at ANL [17] and Dr. Sami Tantawi of SLAC. The goal of this effort is to demonstrate high accelerating gradients in dielectric–loaded structures, and then to develop a compact 20–MeV dielectric–loaded test electron accelerator driven by the 11.424–GHz magnicon output.

The second major application of the magnicon output under the new Agreement will be to the continued study of active microwave pulse compressors. As noted, the first application of the magnicon as a high–power source was to drive a single–channel microwave Active Bragg Compressor that was build by the Institute of Applied Physics in Nizhny Novgorod, Russia in collaboration with Omega–P, Inc. Active pulse compressors have the potential to provide higher levels of pulse compression than passive systems, permitting the use of longer–pulse microwave tubes and reducing the number of separate tubes required to build a linear collider. They can also improve the efficiency of passive systems such as SLED II. The first high–power ABC tests took place in March – April 2001. These tests showed compressed pulses with 14.5–MW peak power in an untriggered mode of operation due to a multipactor discharge on the exterior of the quartz switch tube, and 4.5–MW peak power with a triggered discharge in the gas-filled quartz tube. The occurrence of multipactor discharges on the exterior of the quartz switch tubes limited the output power of the pulse compressor, and showed the necessity for some redesign of the switch region. New quartz discharge tubes designed for 100–MW compressed pulses are being fabricated with larger major radii for placement in weaker rf fields, with TiN coating to inhibit multipactor discharges, and with external gas feeds allowing N_2 pressure changes to adjust the self-breakdown threshold on the interior of the quartz tube. This work will continue under the new Interagency Agreement, with continuing SBIR support to Omega–P, Inc..

The original motivation for this program was to develop a new high–power X–band amplifier tube as a competitor to klystrons for powering future linear colliders. Since the program began, progress on X–band klystrons at SLAC has continued, and they remain the leading candidate to power a future X–band linear collider. However, in terms of power and efficiency, the magnicon remains the only accelerator–class competitor to klystrons in X–band. The final assessment of the experimental success of the program to develop a thermionic magnicon amplifier at 11.4 GHz must await the completion of the magnicon conditioning, which will occur early in the new Interagency Agreement. However, aside from the present level of demonstrated performance of the partially conditioned magnicon, there are a number of additional payoffs from the program. A great deal of progress has been made in magnicon theory and modeling in this program and through the collaboration with Omega–P, Inc. One result of that progress is a separate project at Omega–P to develop a 34–GHz magnicon under DoE SBIR sponsorship. (A successful Ka–band magnicon, unlike a gyroklystron, would be a viable candidate, in terms of power, efficiency, and stability, to power a high–frequency collider at a frequency at which klystrons are not likely to be competitive.) Also as a result of this program, a new high–power 11.424–GHz test facility has been set up at NRL, the only such facility in the U.S. outside of SLAC. This facility will be used for high–power rf component and advanced concepts development, including the development of active pulse compressors and quasioptical power combiners, and for dielectric–loaded accelerator studies relevant to the ongoing X–band rf structure studies at SLAC.

VI. References

[1] M. Karliner, E.V. Kozyrev, I.G. Makarov, O.A. Nezhevenko, G.N. Ostreiko, B.Z. Persov, and G.V. Serdobintsev, "The Magnicon—An Advanced Version of the Gyrocon," *Nucl. Instrum. Methods Phys. Res.*, vol. A269, pp. 459–473, 1988.

[2] O.A. Nezhevenko, "Gyrocons and Magnicons: Microwave Generators with Circular Deflection of the Electron Beam," *IEEE Trans. Plasma Sci.*, vol. 22, pp. 765–772, October 1994

[3] W.M. Manheimer, "Theory and Conceptual Design of a High–Power Highly Efficient Magnicon at 10 and 20 GHz," *IEEE Trans. Plasma Sci.*, vol. 18, pp. 632–645, 1990.

[4] S.H. Gold and G.S. Nusinovich, "Review of High Power Microwave Source Research," *Rev. Sci. Instrum.*, vol. 68, pp. 3945–3974, 1997.

[5] E.V. Kozyrev, O.A. Nezhevenko, A.A. Nikiforov, G.N. Ostreiko, S.V. Shchelkunoff, G.V. Serdobintsev, V.V. Tarnetsky, V.P. Yakovlev, and I.A. Zapryagaev, "Present Status of Budker INP 7 GHz Pulsed Magnicon," in *High Energy Density Microwaves,* AIP Conference Proceedings 474, edited by R.M. Phillips (American Institute of Physics, Woodbury, NY, 1999), pp. 187–194.

[6] S.H. Gold, A.K. Kinkead, A.W. Fliflet, B. Hafizi, and W.M. Manheimer, "Initial Operation of a High Power, Frequency–Doubling X–Band Magnicon Amplifier," *IEEE Trans. Plasma Sci.*, vol. 24, pp. 947–956, June 1996.

[7] V.P. Yakovlev, O.A. Nezhevenko, M.A. LaPointe, J.L. Hirshfield, M.A. Batazova, and G.I. Kuznetsov, "100 MW Electron Gun for a 34.3 GHz Magnicon," in *Proceedings of the 2001 Particle Accelerator Conference*, in press.

[8] A.L. Vikharev, A.M. Gorbachev, O.A. Ivanov, V.A. Isaev, S.V. Kusikov, L. Kolysko, A.G. Litvak, M.I. Petelin, J.L. Hirshfield, O.A. Nezhevenko, and S.H. Gold, "100 MW

Active X–Band Pulse Compressor," in *Proceedings of the 1999 Particle Accelerator Conference, IEEE Catalog No. 99CH36366,* edited by A. Luccio and W. MacKay (IEEE, Piscataway, NJ, 1999), vol. 2, pp. 1474–1476.

[9] S.H. Gold, A.W. Fliflet, A.K. Kinkead, B. Hafizi, O.A. Nezhevenko, V.P. Yakovlev, J.L. Hirshfield, and R. True, "X–Band Magnicon Amplifier for the Next Linear Collider," *Phys. Plasmas*, vol. 4, pp. 1900–1906, May 1997.

[10] V.P. Yakovlev, O.A. Nezhevenko, and R.B. True, "Electron Gun for a High–Power X–band Magnicon Amplifier, in *Proceedings of the 1997 Particle Accelerator Conference, IEEE Catalog No. 97CH36167*, edited by M. Comyn, M.K. Craddock, M. Reiser, and J. Thomson (IEEE, Piscataway, NJ, 1998), vol. 3, pp. 3186–3188.

[11] O.A. Nezhevenko, V.P. Yakovlev, J.L. Hirshfield, E.V. Kozyrev, S.H. Gold, A.W. Fliflet, A.K. Kinkead, R.B. True, and R.J. Hansen, "X–Band Magnicon Amplifier," in *Proceedings of the 1999 Particle Accelerator Conference, IEEE Catalog No. 99CH36366,* edited by A. Luccio and W. MacKay (IEEE, Piscataway, NJ, 1999), vol. 2, pp. 1049–1051.

[12] S.H. Gold, A.K. Kinkead, and O.A. Nezhevenko, "Compact All–Metal High–Vacuum Gate Valve for Microwave Tube Research," *Rev. Sci. Instrum.*, vol. 70, pp. 3770–3773, September 1999.

[13] S.H. Gold, A.K. Kinkead, O.A. Nezhevenko, and V.P. Yakovlev, "System for Measuring the Size of High Current Density Solid Electron Beams *IEEE Trans. Plasma Sci.*, vol. 28, pp. 657–664, June 2000.

[14] S.G. Tantawi and A.E. Vlieks, "Compact X–band High Power Load Using Magnetic Stainless Steel," SLAC–PUB–95–6826, May, 1995.

[15] E.V. Kozyrev, I.G. Makarov, O.A. Nezhevenko, B.Z. Persov, G.V. Serdobintsev, S.V. Shchelkunoff, V.V. Tarnetsky, V.P. Yakovlev, and I.A. Zapryagaev, Part. Accel., vol. 52, pp. 55–64, 1996.

[16] V. Yakovlev, O. Danilov, O. Nezhevenko, and V. Tarnetsky, "Numerical Simulation of Magnicon Amplifier," in *Proceedings of the 1995 Particle Accelerator Conference*, (Institute of Electrical and Electronics Engineers, Piscataway, NJ, 1995), vol. III, pp. 1569–1570.

[17] S.H. Gold and W. Gai, "High–Power Testing of 11.424–GHz Dielectric–Loaded Accelerating Structures," in *Proceedings of the 2001 Particle Accelerator Conference*, in press.

Appendix I

Scientific Publications (May 1995–May 2001)

Journal Articles

1. "Theory of Competition between Synchronous and Nonsynchronous Modes in a Magnicon Output Cavity," by A.W. Fliflet and S.H. Gold, Phys. Plasmas, vol. 2, pp. 1760–1765, May 1995.
2. "Initial Operation of a High Power, Frequency–Doubling X–Band Magnicon Amplifier," by Steven H. Gold, Allen K. Kinkead, Arne W. Fliflet, Bahman Hafizi, and Wallace M. Manheimer, IEEE Trans. Plasma Sci., vol. 24, pp. 947–956, June 1996.
3. "Mode Competition in Fourth–Harmonic Magnicon Amplifiers," by Arne W. Fliflet and Steven H. Gold, IEEE Trans. Plasma Sci., vol. 24, pp. 957–963, June 1996.
4. "Beam Loading in Magnicon Deflection Cavities," by B. Hafizi and S.H. Gold, IEEE Trans. Plasma Sci., vol. 25, pp. 53–59, February 1997.
5. "X–Band Magnicon Amplifier for the Next Linear Collider," by Steven H. Gold, Arne W. Fliflet, Allen K. Kinkead, B. Hafizi, Oleg A. Nezhevenko, Viacheslav P. Yakovlev, Jay L. Hirshfield, and Richard True, Phys. Plasmas, vol. 4, pp. 1900–1906, May 1997.
6. "Review of High Power Microwave Source Research [Invited Review Paper]," by Steven H. Gold and Gregory S. Nusinovich, Rev. Sci. Instrum., vol. 68, pp. 3945–3974, November 1997.
7. "Compact All–Metal High–Vacuum Gate Valve for Microwave Tube Research," by Steven H. Gold, Allen K. Kinkead, and Oleg A. Nezhevenko, Rev. Sci. Instrum., vol. 70, pp. 3770–3773, September 1999.

8. "System for Measuring the Size of High Current Density Solid Electron Beams," by S.H. Gold, A.K. Kinkead, O.A. Nezhevenko, and V.P. Yakovlev, IEEE Trans. Plasma Sci., vol. 28, pp. 657–664, June 2000.

Conference Proceedings Papers

1. "Initial Operation of an X–Band Magnicon Amplifier Experiment," by S.H. Gold, A.K. Kinkead, A.W. Fliflet, and B. Hafizi, in Proceedings of the 1995 Particle Accelerator Conference, IEEE Catalog No. 95CH35843 (IEEE, Piscataway, NJ, 1996), vol. 3, pp. 1611–1613.
2. "Development of an X–Band Magnicon Amplifier for the Next Linear Collider," by S.H. Gold, A.W. Fliflet, A.K. Kinkead, B. Hafizi, O.A. Nezhevenko, V.P. Yakovlev, J.L. Hirshfield, and R. True, in Advanced Accelerator Concepts, AIP Conference Proceedings 398, edited by S. Chattopadhyay, J. McCullough, and P. Dahl (American Institute of Physics, New York, 1997), pp. 832–841.
3. "X–Band Magnicon Amplifier for the Next Linear Collider," by S.H. Gold, A.W. Fliflet, A.K. Kinkead, B. Hafizi, O.A. Nezhevenko, V.P. Yakovlev, J.L. Hirshfield, R. True, and R.J. Hansen, in Proceedings of the 1997 Particle Accelerator Conference, IEEE Catalog No. 97CH36167, edited by M. Comyn, M.K. Craddock, M. Reiser, and J. Thomson (IEEE, Piscataway, NJ, 1998), vol. 3, pp. 3153–3155.
4. "Development of a 50 MW Magnicon Amplifier at 11.4 GHz," by S.H. Gold, A.W. Fliflet, A.K. Kinkead, B. Hafizi, O.A. Nezhevenko, V.P. Yakovlev, J.L. Hirshfield, R. True, and R.J. Hansen, in Conference Digest—Twenty–Second International Conference on Infrared and Millimeter Waves, edited by H.P. Freund (available from R.H. Jackson, Code 6840, Naval Research Laboratory, Washington, DC 20375, 1997), pp. 309–310.

5. “Status Report on the 11.424 GHz Magnicon Amplifier,” by S.H. Gold, O.A. Nezhevenko, V.P. Yakovlev, A.K. Kinkead, A.W. Fliflet, E.V. Kozyrev, R. True, R.J. Hansen, and J.L. Hirshfield, in High Energy Density Microwaves, AIP Conference Proceedings 474, edited by R.M. Phillips (American Institute of Physics, Woodbury, NY, 1999), pp. 179–186.

6. “X–Band Magnicon Amplifier,” by O.A. Nezhevenko, V.P. Yakovlev, J.L. Hirshfield, E.V. Kozyrev, S.H. Gold, A.W. Fliflet, A.K. Kinkead, R.B. True, and R.J. Hansen, in Proceedings of the 1999 Particle Accelerator Conference, IEEE Catalog No. 99CH36366, edited by A. Luccio and W. MacKay (IEEE, Piscataway, NJ, 1999), vol. 2, pp. 1049–1051.

7. “100 MW Active X–Band Pulse Compressor,” by A.L. Vikharev, A.M. Gorbachev, O.A. Ivanov, V.A. Isaev, S.V. Kusikov, L. Kolysko, A.G. Litvak, M.I. Petelin, J.L. Hirshfield, O.A. Nezhevenko, and S.H. Gold, in Proceedings of the 1999 Particle Accelerator Conference, IEEE Catalog No. 99CH36366, edited by A. Luccio and W. MacKay (IEEE, Piscataway, NJ, 1999), vol. 2, pp. 1474–1476.

8. “Summary Report of Working Group 6—Millimeter–Wave Sources,” by G.S. Nusinovich and S.H. Gold, in Advanced Accelerator Concepts—Ninth Workshop, Santa Fe, NM, 10–16 June 2000, AIP Conference Proceedings 569, edited by P.L. Colestock and S. Kelly (American Institute of Physics, Melville, NY, 2001), pp. 65–76.

9. “CARM–Klystron Amplifier for Accelerator Applications,” by S.H. Gold and A.W. Fliflet, in Advanced Accelerator Concepts—Ninth Workshop, Santa Fe, NM, 10–16 June 2000, AIP Conference Proceedings 569, edited by P.L. Colestock and S. Kelly (American Institute of Physics, Melville, NY, 2001), pp. 695–701.

10. “High–Power Testing of 11.424–GHz Dielectric–Loaded Accelerating Structures,” by S.H. Gold and W. Gai, in Proceedings of the 2001 Particle Accelerator Conference, in press.

11. "Status of X–Band Pulsed Magnicon Project," by O.A. Nezhevenko, V.P. Yakovlev, J.L. Hirshfield, S.H. Gold, A.W. Fliflet, and A.K. Kinkead, in Proceedings of the 2001 Particle Accelerator Conference, in press.

Technical Reports

1. "X–Band Magnicon Amplifier Research at the Naval Research Laboratory," by S.H. Gold, B. Hafizi, and A.W. Fliflet, *NRL Memorandum Report 6793–95–7666* (1995).

2. "Development of a Thermionic Magnicon Amplifier at 11.4 GHz — Technical Progress Report for Period 16 May 1994 – 31 December 1995," by S.H. Gold, A.W. Fliflet, and W.M. Manheimer, Report No. DOE/ER/40861–1.

3. "Initial Operation of a High Power, Frequency–Doubling X–Band Magnicon Amplifier," by S.H. Gold, A.K. Kinkead, A.W. Fliflet, B. Hafizi, and W.M. Manheimer, *NRL Memorandum Report 6793–96–7788* (1996).

4, "Development of a Thermionic Magnicon Amplifier at 11.4 GHz — Technical Progress Report for Period 1 January 1996 – 31 December 1996," by S.H. Gold, A.W. Fliflet, and W.M. Manheimer, Report No. DOE/ER/40861–2.

5. "Design of a High Power Thermionic Magnicon Amplifier at 11.4 GHz," by S.H. Gold, O.A. Nezhevenko, V.P. Yakovlev, and B. Hafizi, *NRL Memorandum Report 7857* (1996).

6. "Development of a Thermionic Magnicon Amplifier at 11.4 GHz — Technical Progress Report for Period 1 January 1997 – 1 December 1997," by S.H. Gold, A.W. Fliflet, and W.M. Manheimer, Report No. DOE/ER/40861–3.

7. "Development of a Thermionic Magnicon Amplifier at 11.4 GHz — Technical Progress Report for Period 31 January 1997 – 15 February 1999," by S.H. Gold and A.W. Fliflet, Report No. DOE/ER/40861–4.

8. "Development of a Thermionic Magnicon Amplifier at 11.4 GHz — Technical Progress Report for Period 15 February 1999 – 31 December 1999," by S.H. Gold and A.W. Fliflet, Report No. DOE/ER/40861–5.
9. "Development of a Thermionic Magnicon Amplifier at 11.4 GHz — Technical Progress Report for Period 1 January 2000 – 31 December 2000," by S.H. Gold and A.W. Fliflet, Report No. DOE/ER/40861–6.
10. "Development of a Thermionic Magnicon at 11.4 GHz," by S.H. Gold, in "Advanced Technology Research and Development 2000," DoE/SC–0032, edited by D. Sutter and B. Strauss, (Department of Energy, Germantown, MD, 2001), pp. 57–60.

Invited Papers

1. "Development of an X–band Magnicon Amplifier for the Next Linear Collider—Cold Cathode Experiments and a Thermionic Design Study," by S.H. Gold, B. Hafizi, A.W. Fliflet, A.K. Kinkead, O.A. Nezhevenko, V.P. Yakovlev, and R.B. True, presented at the Twenty–Third IEEE International Conference on Plasma Science, 3–5 June 1996, Boston, MA. [*Conference Record–Abstracts, IEEE Catalog No. 96CH35939*, p. 231.]
2. "Developments in the NRL X–Band Magnicon Program," by S.H. Gold, presented at the Thirty–Eighth Annual Meeting of the Division of Plasma Physics, American Physical Society, 11–15 November 1996, Denver, CO. [*Bull. Amer. Phys. Soc.*, vol. 41, p. 1474, 1996.]

Contributed Conference Papers

1. "Initial Operation of an X–Band Magnicon Amplifier Experiment," by S.H. Gold, B. Hafizi, and A.W. Fliflet, presented at the 1995 Particle Accelerator Conference, 1–5 May 1995, Dallas, TX. [postdeadline]

2. “Recent Results from the NRL X–Band Magnicon Amplifier Experiment,” by S.H. Gold, A.W. Fliflet, and B. Hafizi, presented at the Twenty–Second IEEE International Conference on Plasma Science, 5–8 June 1995, Madison, WI. [*Conference Record–Abstracts, IEEE Catalog No. 95CH35796,* pp. 246–247.]

3. “Mode Competition in Harmonic Magnicon Amplifiers,” by A.W. Fliflet and S.H. Gold, presented at the Twenty–Second IEEE International Conference on Plasma Science, 5–8 June 1995, Madison, WI. [*Conference Record–Abstracts, IEEE Catalog No. 95CH35796,* p. 247.]

4. “Field Analysis of Beam Loading and Detuning in Magnicon Deflection Cavities,” by B. Hafizi and S.H. Gold, presented at the Twenty–Second IEEE International Conference on Plasma Science, 5–8 June 1995, Madison, WI. [*Conference Record–Abstracts, IEEE Catalog No. 95CH35796,* pp. 279–280.]

5. “Initial Operation of the NRL X–Band Magnicon Amplifier Experiment,” by S.H. Gold, A.K. Kinkead, B. Hafizi, and A.W. Fliflet, presented at the Thirty–Seventh Annual Meeting of the Division of Plasma Physics, American Physical Society, 6–10 November 1995, Louisville, KY. [*Bull. Amer. Phys. Soc.*, vol. 40, pp. 1675–1676, 1995.]

6. “Field Analysis of Beam Loading in Magnicon Deflection Cavities,” by B. Hafizi and S.H. Gold, presented at the Thirty–Seventh Annual Meeting of the Division of Plasma Physics, American Physical Society, 6–10 November 1995, Louisville, KY. [*Bull. Amer. Phys. Soc.*, vol. 40, p. 1676, 1995.]

7. “Development of an X–Band Magnicon Amplifier for the Next Linear Collider,” by S.H. Gold, B. Hafizi, O.A. Nezhevenko, V.P. Yakovlev, A.K. Kinkead, A.W. Fliflet, J.L. Hirshfield, and R. True, presented at the Seventh Workshop on Advanced Accelerator Concepts, 12–18 October 1996, Lake Tahoe, CA. [*Advanced Accelerator Concepts,* AIP Conference Proceedings 398, p. 832.]

8. "The NRL X–Band Thermionic Magnicon Amplifier Experiment," by S.H. Gold, A.W. Fliflet, O.A. Nezhevenko, V.P. Yakovlev, J.L. Hirshfield, B. Hafizi, A.K. Kinkead, and R. True, presented at the 1997 Particle Accelerator Conference, 12–16 May 1997, Vancouver, B.C., Canada. [*Bull. Amer. Phys. Soc.*, vol. 42, p. 1272, 1997.]

9. "Development of a Thermionic Magnicon Amplifier at 11.4 GHz," by S.H. Gold, B. Hafizi, A.W. Fliflet, A.K. Kinkead, O.A. Nezhevenko, V.P. Yakovlev, J.L. Hirshfield, and R. True, presented at the Twenty–Fourth IEEE International Conference on Plasma Science, 19–22 May 1997, San Diego, CA. [*Conference Record–Abstracts, IEEE Catalog No. 97CH36085,* pp. 222–223.]

10. "Development of a 50 MW Magnicon Amplifier at 11.4 GHz," by S.H. Gold, A.W. Fliflet, A.K. Kinkead, B. Hafizi, O.A. Nezhevenko, V.P. Yakovlev, J.L. Hirshfield, and R. True, presented at the Twenty–Second International Conference on Infrared and Millimeter Waves, 20–25 July 1997, Wintergreen, VA. [*Conference Digest,* pp. 309–310.]

11. "X–Band Thermionic Magnicon Amplifier Experiment," by S.H. Gold, A.W. Fliflet, O.A. Nezhevenko, V.P. Yakovlev, J.L. Hirshfield, B. Hafizi, A.K. Kinkead, R. True, and R. Hansen, presented at the Thirty–Ninth Annual Meeting of the Division of Plasma Physics, American Physical Society, 17–21 November 1997, Pittsburgh, PA. [*Bull. Amer. Phys. Soc.*, vol. 42, p. 1904, 1997.]

12. "Development of a High–Power Magnicon Amplifier at 11.424 GHz," by S.H. Gold, O.A. Nezhevenko, V.P. Yakovlev, A.K. Kinkead, E.V. Kozyrev, A.W. Fliflet, B. Hafizi, R. True, R.J. Hansen, and J.L. Hirshfield, presented at the Twenty–Fifth IEEE International Conference on Plasma Science, 1–4 June 1998, Raleigh, NC. [*Conference Record–Abstracts, IEEE Catalog No. 98CH36221,* p. 194.]

13. "Progress Report on the NRL/Omega–P 11.4 GHz Magnicon Amplifier Project," by S.H. Gold, O.A. Nezhevenko, V.P. Yakovlev, A.K. Kinkead, A.W. Fliflet, E.V. Kozyrev, R. True, R.J. Hansen, and J.L. Hirshfield, presented at the Eighth Workshop on Advanced Accelerator Concepts, 5–11 July 1998, Baltimore, MD.

14. "Status Report on the 11.424 GHz Magnicon Amplifier," by S.H. Gold, O.A. Nezhevenko, V.P. Yakovlev, A.K. Kinkead, A.W. Fliflet, E.V. Kozyrev, R. True, R.J. Hansen, and J.L. Hirshfield, presented at RF98, 5–9 October 1998, Watsonville, CA [*AIP Conference Proceedings 474*, pp. 179–186.]

15. "Development of an 11.424 GHz Magnicon Amplifier," by S.H. Gold, O.A. Nezhevenko, V.P. Yakovlev, A.K. Kinkead, A.W. Fliflet, R. True, R.J. Hansen, E.V. Kozyrev, and J.L. Hirshfield, presented at the Fortieth Annual Meeting of the Division of Plasma Physics, American Physical Society, 16–20 November 1998, New Orleans, LA. [*Bull. Amer. Phys. Soc.*, vol. 43, p. 1835, 1998.]

16. "X–Band Magnicon Amplifier," by O.A. Nezhevenko, V.P. Yakovlev, J.L. Hirshfield, S.H. Gold, A.W. Fliflet, A.K. Kinkead, R. True, R.J. Hansen, and E.V. Kozyrev, presented at the 1999 Particle Accelerator Conference, 29 March – 2 April 1999, New York, NY. [*Conference Proceedings,* pp. 1049–1051.]

17. "100 MW Active X–Band Pulse Compressor," by A.L. Vikharev, A.M. Gorbachev, O.A. Ivanov, V.A. Isaev, S.V. Kusikov, A.L. Kolysko, A.G. Litvak, M.I. Petelin, J.L. Hirshfield, O.A. Nezhevenko, and S.H. Gold, presented at the 1999 Particle Accelerator Conference, 29 March – 2 April 1999, New York, NY. [*Conference Proceedings,* pp. 1474–1476.]

18. “Analyzer for Profile Measurements of a Beam from a Magnicon Electron Gun,” by S.H. Gold, A.K. Kinkead, A.W. Fliflet, R. True, R.J. Hansen, and J.L. Hirshfield, presented at the Twenty–Sixth IEEE International Conference on Plasma Science, 20–24 June 1999, Monterey, CA. [*Conference Record–Abstracts, IEEE Catalog No. 99CH36297,* p. 168.]

19. “Microwave and Beam Diagnostics for an 11.424 GHz Magnicon,” by S.H. Gold, A.W. Fliflet, O.A. Nezhevenko, V.P Yakovlev, J.L. Hirshfield, E.V. Kozyrev, and A.K. Kinkead, presented at the Forty–First Annual Meeting of the Division of Plasma Physics, American Physical Society, 15–19 November 1999, Seattle, WA. [*Bull. Amer. Phys. Soc.*, vol. 44, p. 296, 1999.]

20. “X–Band Pulsed Magnicon for Next Linear Collider,” by O.A. Nezhevenko, V.P Yakovlev, J.L. Hirshfield, E.V. Kozyrev, S.H. Gold, A.W. Fliflet, and A.K. Kinkead, presented at the Forty–First Annual Meeting of the Division of Plasma Physics, American Physical Society, 15–19 November 1999, Seattle, WA. [*Bull. Amer. Phys. Soc.*, vol. 44, p. 252, 1999.]

21. “X–Band Magnicon Amplifier Experiment,” by S.H. Gold, A.W. Fliflet, O.A. Nezhevenko, V.P. Yakovlev, J.L. Hirshfield, E.V. Kozyrev, and A.K. Kinkead, presented at ICOPS 2000—The Twenty–Seventh IEEE International Conference on Plasma Science, 4–7 June 2000, New Orleans, LA. [*Conference Record–Abstracts, IEEE Catalog No. 00CH37087*, p. 173.]

22. “CARM–Klystron Amplifier for Accelerator Applications,” by S.H. Gold and A.W. Fliflet, presented at AAC 2000—The Ninth Workshop on Advanced Accelerator Concepts, 10–16 June 2000, Santa Fe, New Mexico. [Conference Proceedings, pp. 695–701.]

23. "X–Band Magnicon Amplifier Experiment," by S.H. Gold, A.W. Fliflet, O.A. Nezhevenko, V.P. Yakovlev, J.L. Hirshfield, A.K. Kinkead, R.L. Ives, and Y.M. Mizuhara, presented at the Forty–Second Annual Meeting of the Division of Plasma Physics, American Physical Society, 23–27 October 2000, Québec City, Canada. [*Bull. Amer. Phys. Soc.*, vol. 45, p. 136, 2000.]

24. "X–Band Magnicon Amplifier Experiment," by S.H. Gold, A.W. Fliflet, O.A. Nezhevenko, V.P. Yakovlev, J.L. Hirshfield, and A.K. Kinkead, presented at Pulsed Power Plasma Science 2001, the joint meeting of the Twenty–Eighth IEEE International Conference on Plasma Science and the Thirteenth IEEE International Pulsed Power Conference, 17–22 June 2001, Las Vegas, NM. [*Conference Record–Abstracts, IEEE Catalog No.01CH37255,* p. 515.]

25. "High–Power Testing of an 11.4–GHz Dielectric–Loaded Accelerating Structure," by S.H. Gold and W. Gai, presented at PAC 2001, the 2001 Particle Accelerator Conference, 18–22 June 2001, Chicago, IL.

26. "Status of X–Band Pulsed Magnicon Project," by O.A. Nezhevenko, V.P. Yakovlev, J.L. Hirshfield, S.H. Gold, A.W. Fliflet, and A.K. Kinkead, presented at PAC 2001, the 2001 Particle Accelerator Conference, 18–22 June 2001, Chicago, IL.